New Perspectives for the Structure and Development Mecanism of the Arctic Cyclones

November 2016

Takuro AIZAWA

New Perspectives for the Structure and Development Mecanism of the Arctic Cyclones

A Dissertation Submitted to
the Graduate School of Life and Environmental Sciences,
the University of Tsukuba
in Partial Filfillment of the Requirements
for the Degree of Doctor of Philosophy in Science
(Doctoral Program in Geoenvironmental Sciences)

Takuro AIZAWA

Abstract

Arctic cyclones are unique low pressure systems in the Arctic, which are different from the tropical cyclones and the mid-latitude cyclones. The axisymmetric structures of two major Arctic cyclones which appeared in June 2008 and August 2012 are examined based on the cylindrical coordinate system around the Arctic cyclone. The result demonstrates that the Arctic cyclone has a deep barotropic cyclonic circulation, a secondary circulation in the troposphere, a downdraft at the lower stratosphere, a coupling of a warm core at the lower stratosphere and a cold core in the troposphere, and a deep tropopause folding above the cyclone center. The horizontal scale of the Arctic cyclone reaches 5000 km in diameter which is one of the largest cyclones found on the Earth. Note that the cyclone of June 2008 appears showing axisymmetric cyclonic circulations at the surface level. The cyclone of 2012 is characterized by the structure change from the cold core to the warm core at the lower stratosphere, indicating a shift from the ordinary baroclinic cyclone to the typical Arctic cyclone. Although additional studies are needed, a schematic diagram of the Arctic cyclone is proposed in this study.

And in this study, we conducted a numerical simulation of a rapid development of an Arctic cyclone that appeared in June 2008 using a cloud resolving global model, Nonhydrostatic ICosahedral Atmospheric Model (NICAM). We investigated the three dimensional structure and intensification mechanism of the simulated Arctic cyclone that developed to the minimum sea level pressure of 971 hPa in the model. According to the result, the Arctic cyclone indicates a barotropic structure with a warm core in the lower stratosphere and a cold core in the troposphere. The development of the Arctic cyclone is accompanied by an intense mesoscale cyclone showing baroclinic structure with a marked local arctic front. The upper level warm core of the Arctic cyclone is formed by

an adiabatic heating associated with the downdraft in the lower stratosphere. The rapid development of the Arctic cyclone is caused by the combination of the intensification of the upper level warm core and the merging with the baroclinically growing mesoscale cyclone in the lower level. The merging of the Arctic cyclone and mesoscale cyclone and the vertical vortex coupling with the upper air polar vortex are the most important mechanisms for the rapid development of the Arctic cyclone.

This study proposed life cycle of the Arctic cyclones. The thermal structure of the Arctic cyclone is very stable having an upper warm core and a lower cold core. This thermal stability is one of the factors to long lasting for the Arctic cyclones. Here, we explain the further reason. The life cycle of the Arctic cyclone is able to classify in following five phases. The first stage of the Arctic cyclone indicates that the upper polar vortex accompanied with a warm core intensifies due to the adiabatic warming by downdraft or static stability in the troposphere weakens by some mechanism, which produces the surface cyclone. The second stage indicates that as the adiabatic warming intensifies, the surface cyclone develops indicating strong low pressure. The third stage is that as the surface cyclone intensifies, the updraft in the troposphere becomes gradually dominant indicating cold core intensifying, which decreases the surface pressure of the cyclone. The fourth stage of the life cycle is that the cyclone often merges with other frontal cyclones originated in the Arctic front or the mid-latitudes, indicating more intensification of the pre-existing Arctic cyclone. The structures after merging inherit the structures of the Arctic cyclones. The final stage is that the lower stratospheric downdraft and the tropospheric updraft are balanced each other, indicating the surface cyclone maintains long time. Therefore, the Arctic cyclone can have long time scale about life cycle. Thus, the life cycle of the Arctic cyclone is unique, and which is different from the life cycle of the mid-latitude cyclones.

Keyword

Arctic cyclone, polar vortex, baroclinic cyclone, merging, thermal structure, dynamical structure, adiabatic warming by downdraft, life cycle

CONTENTS

LIST of TABLES

LIST of FIGURES

1 Introduction

Cyclones have diversity. The cyclones play a primary role in the weather and the climate from the tropics to the poles. The meteorologists roughly distinguish between tropical cyclone and extratropical cyclone, which are seen in the weather map at the lower levels, such as sea level. When the meteorologists call a cyclone, most of cases are mid-latitude cyclones as synoptic disturbances. Extratropical cyclones are mainly driven by the strong temperature and moisture gradients across the polar front and often develop in the baroclinic regions over, for example, the Gulf Stream or Kuroshio Current in the Northern Hemisphere. But, there are many kind of cyclones appearing in the extra-tropics. The cyclones develop in various ways along the environmental conditions. As a region of extra-tropics covers the wide part on the Earth, it allows that the cyclones have diversity.

When we see a weather map at upper level, for example 500 hPa, we can find usually a large scale low pressure system centered on the Arctic. Meteorolgist call the large low pressure as the polar vortex, which drives the atmospheric general circulation indicating jet streams, which create the mid-latitude weather system. The polar vortex is the largest cyclones appearing on the Earth. The jet stream separates the cold Arctic from the warm tropics, and the polar vortex is filled with cold air mass. Therefore, viewing from the aspect of cyclone, the thermal structure of the polar vortex is cold core. Cold vortex as a cut-off low pressure system is often seen in the weather map of same level, which is separated by some mechanism from the polar vortex. Thus, the cold vortex indicates similar thermal structure as the polar vortex. Mid-latitude cyclones and traveling highs are transfered by the zonal jet stream accompanied with the polar vortex. Therefore, the polar vortex is a primary cyclone on the Earth.

1.1 Mid-latitude cyclone

Frontal cyclones in the mid-latitude have been studied since 1920s by many researchers. Some conceptual models for the cyclone were proposed in the long history of studies. A theory about the life cycle of frontal cyclone by Bjerknes and Solberg (1922) is well known. The frontal cyclone develops in four phases. The initial phase of cyclone formation is given by two oppositely directed currents of different temperatures, the cyclone develops with a couple of warm front and cold front, the fronts occlude with the cyclone developing, and the cyclone dissipates with time in the cold air mass. A number of intensive observing campaings conducted to understand rapid cyclogenesis, including the Fronts and Atlantic Storm-Track EXperiment (FASTEX; Joly et al. 1997, 1999) and the Experiment on Rapidly Intensifying Cyclone over the Atlantic (ERICA; Hadlock and Kreitzberg 1988). Shapiro and Keyser (1990) proposed a new conceptual model for the development of the frontal cyclone based on those observation. The thermal structure of the cyclone in the mature stage becomes a warm core via the seclusion process of the warm air by their model. Figure 1 shows the conceptual models of the life cycle of the frontal cyclone by Bjerknes and Solberg (1922) and Shapiro and Keyser (1990) from Schults et al. (1998). The development mechanisms and structures of the cyclones have been fully understood by the efforts of the many researchers based on those two conceptual models. The development of the frontal cyclone involving the occlusion process is summarized well by Browning and Roberts (1994) or Schultz and Vaughan (2011). Hewson and Neu (2015) segmentalized in more phases for the conceptual model of Shapiro and keyser (1990). Catto (2016) reviewed very well about the previous studies with respect to the extratropical cyclone classification. Both conceptual models are particularly powerful to explain the development of the cyclones, but which are only directed to the frontal cyclones in mid-latitudes.

1.2 Arctic cyclone

The cyclone activity is found not only in the mid-latitude but also in the Arctic. The cyclones appearing in the Arctic is called the Arctic cyclones conventionally. The cyclone activity over the Arctic Ocean is the strongest in summer season (Serreze and Barrett 2007; Simmonds et al. 2008). Zhang et al. (2004) revealed that the summer Arctic cyclones are weaker but longer lasting compared with that of any other seasons by a statistical study. They also showed the two types of Arctic cyclones with their origins in the mid-latitudes and in the Arctic.

The arctic front located between the continent and the iced ocean can play a major role in the Arctic cyclogenesis (e.g., Ledrew 1984, 1987, 1989; Serreze et al. 2001). A recent observational study by Inoue and Hori (2011) showed that a strong baroclinicity exists along the edge of the sea ice where is called the merginal ice zone, and its baroclinicity plays a key role in the Arctic cyclogenesis in the same way as the mid-latitude cyclones. Thus, a number of previous studies identified the cyclones in the Arctic as mid-latitude cyclones generated in high latitudes. However, baroclinicity or vertical wind shear and horizontal temperature gradient is relatively weak in the high latitudes where the Arctic cyclones are most common. Some recent studies provided new insights into the understandings of Arctic cyclone. Tanaka et al. (2012) revealed by the case studies for the long-lived Arctic cyclones that the surface cyclone connects to the upper polar vortex producing a deep barotropic vortex. The thermal structure of the cyclone is characterized by a coupling of a warm core at the lower stratosphere and a cold core in the troposphere. They also noted that the characteristic thermal and the vortical structures are maintained throughout a life cycle. Aizawa et al. (2014) analyzed the same thermal structure and a deep wide-spread tropopause folding related to the intensification of the polar vortex, which is cleared more systematically in this

study. Those structural features are different from the mid-latitude cyclone and the tropical cyclones. The tropopause folding is a common structure for both the Arctic cyclone and the mid-latitude cyclone. However, the upper tropopause folding of the Arctic cyclone is located over the cyclone center, and that of the mid-latitude cyclone is located at the back side of the cyclone center (e.g., Shapiro and Keyser 1986; Hakim et al. 1995; Browning 1997; Wernli et al. 2002; Posselt and Martin 2004). But, the three dimensional stereoscopic structure of the Arctic cyclones was not investigated by their studies. The typical structure of mid-latitude cyclones and tropical cyclones including fine scale structure has been considerably understood by a lot of the frontal studies. The purpose of this study is to show the three dimensional structure of the typical Arctic cyclones.

Since there are only few studies for the individual cyclone system (e.g., LeDrew 1984, 1987), the Arctic cyclogenesis and the development mechanism are still unknown. Previous studies were conducted to understand the summer cyclones, most of them are statistical and climatological studies (e.g., Zhang et al. 2004; Serreze and Barrett 2007; Simmonds et al. 2008). Therefore, the detail investigatation of the mechanisms of Arctic cyclogenesis is also focused on this study.

1.3 Relationship between Arctic cyclone and Arctic climate

Rapidly changing arctic climate system in recent decades has attracted the interest of a large number of scientists working on the Arctic. Quite many mechanisms constructing the arctic climate have been elucidated by previous studies, but there are still many unsolved questions today. One of the questions is to explain how the Arctic cyclone is influencing the arctic climate system in summer. Although there are many studies on the synoptic scale phenomena in the summer Arctic, not many studies were conducted

on the unique features of the Arctic cyclone. Serreze and Barrett (2007) showed that the cyclone activity over the Arctic Ocean is the strongest in summer during the course of a year. Similar conclusions were obtained by Simmonds et al. (2008). Large portion of the Arctic Ocean is covered by sea ice in summer, and a number of recent studies showed that the sea ice concentration has been decreasing (e.g., Cavalieri et al. 2003; Stroeve et al. 2007). Thus, the summer cyclone activity in the Arctic may have considerable influences on the sea ice extent. Moreover, if the summer cyclones over the Arctic Ocean continue for a long time, they may affect not only the sea ice distribution but also the short-term climate such as monthly mean temperature and precipitation. Therefore, it is quite important for the Arctic climate system to understand the summer cyclones in the Arctic.

According to an observational study of Rigor et al. (2000), the surface air temperature around the central Arctic Ocean in summer is approximately 0 ℃ in climate. It is known that the temperature in summer is relatively lower when many cyclones appear over the Arctic Ocean compared to the normal summer. Simmonds and Keay (2009) revealed the relationship between the summer cyclone activity over the Arctic Ocean and the sea ice distributions. In August 2012, the greatest Arctic cyclone in record was generated in the Arctic, which had a great impact on the sea ice distribution (e.g., Simmonds and Rudeva 2012). The minimum sea ice extent in history was recorded in September 2012 after that event. Therefore, it is important to understand the three dimensional structure and life cycle of the cyclones in the Arctic, which will have an impact on the research of the Arctic environment.

1.4 Numerical Models and Arctic climate

Modeling studies of the Arctic cyclone are almost absent. To assist our understanding of the Arctic cyclones, a numerical model is useful to fill the absence of the observations over the Arctic Ocean and the uncertainty of the reanalysis data, because the model atmosphere has a consistency in its dynamics and physics. A new atmospheric general circulation model called Nonhydrostatic ICosahedral Atmospheric Model (NICAM) is developed and improved by the Center for Climate System Research, University of Tokyo and Frontier Research Center for Global Change/Japan Agency for Marine-Earth Science and Technology (Satoh et al. 2008). There are two remarkable features in the high-resolution NICAM. First, the NICAM has a capability to calculate the vertical velocity and the cloud system directly. Second, the NICAM is characterized by quasi-homogeneous grid system without the lateral boundaries.

It is well known that the NICAM performs well on the simulation of MJO and tropical cyclones in the tropics. The cloud process strongly influences the development of the intense cyclone in the mid-latitudes. Precipitation and cloud structure in mid-latitude cyclone was investigated well by Fields and Wood (2007). The formation of the cloud systems over the Arctic Ocean is one of the unsolved problems of the arctic weather. Since the NICAM has a capability of resolving the clouds, it may reproduce the cloud systems and the precipitation distributions well over the Arctic. Therefore, the NICAM is a quite useful model to understand the arctic weather. It is important for understanding the climate system of the Arctic to elucidate the mechanisms of the life cycle of the summer Arctic cyclones. The purpose of the present study is to understand the mechanisms of the development and the maintenance of the Arctic cyclone using the high resolution global model NICAM.

1.5 The purpose of this study

From Catto (2016), the extratropical cyclones i.e. mid-latitude cyclones were classified by the various ways, including observation, satellite classification, airstream analysis and synoptic-dynamic classification. Those classifications are based on the observational analyses, the numerical simulations, theoretical and mathematical studies. Thus, the classifications of the mid-latitude frontal cyclone have been conducting in the various previous studies (e.g., Pettersen and Smebye 1973; Throncroft et al. 1993; Deveson et al. 2002). However, the classification of the cyclone appearing in the Arctic has not been conducted in the history of cyclone study. As mentioned above, the structure and development mechanism of Arctic cyclone is less understanding than the other cyclone systems. The purpose of this study is to clear the Arctic cyclone about the structure and development mechanism from the analysis of the reanalysis data and the numerical simulation.

In the near future, the Arctic cyclones will be classified as a same rank as mid-latitude cyclones and tropical cyclones, as distinct from the extratropical cyclones through a lot of the future works. As the first step of Arctic cyclone classification, the goal of this study is to propose the structure model and the conceptual model of the Arctic cyclone's life cycle.

2 Methodology

2.1 Explanation of cyclones

The Arctic cyclones chosen in this study are cases of June 2008 (Tanaka et al. 2012; Aizawa et al. 2014; Aizawa and Tanaka 2016) and August 2012 (Simmonds and Rudeva 2012; Aizawa and Tanaka 2016). Figure 2 shows the satellite imagenary on 5 August 2012 of an Arctic cyclone which is in the mature stage. The Arctic cyclone locates on the central Arctic Ocean indicating spiral clouds band with mixed colors of brightness white and the gray. To capture of Arctic cyclone by satellite is difficult due to the roughness of time resolution or the weaker color contrast between sea ice and clouds. Despite their difficuties, the Arctic cyclones are rearly cuptured by satellites or shipboards. The Arctic cyclone of August 2012 (case 2012) is one of the precious cases.

The original data used this study are the reanalysis data of JRA-25/JCDAS (Japanese 25year Reanalysis/JMA Climate Data Assimilation System; JMA: Japan Meteorological Agency). We compared the cyclones of JRA-25/JCDAS to those of more recent reanalysis JRA-55 (Japanese 55year Reanalysis) on the SLP field, and we confirmed that there are no differences between the reanalysis data through the life cycles of cyclones. Therefore, the reanalysis of JRA-25/JCDAS is enough data to analyze the cyclone in detail.

We tracked the minima of sea level pressure field using interpotating method described below, and presumed them as the cyclone centers. Figure 3 illustrates the tracks and the central pressures of the Arctic cyclones. The Arctic cyclone of June 2008 (case 2008) emerged above the Arctic Ocean at 00Z, 10 June 2008, after then roamed around the Arctic Ocean for more than two weeks. The cyclone is the one of the most persistent cases lasting 18 days. The cyclone appeared at 00Z, 10 June 2008, and had been rapidly intensifying for 30 hours from 00Z, 21 June 2008 to 06Z, 22 June 2008. The minimum

sea level pressure of the cyclone fell below 980 hPa at that time. The minimum pressure in the life cycle is 977 hPa. This individual cyclone is used in numerical simulation by NICAM. We show in Fig. 4 the sea level pressure (SLP) of the arctic region on 00Z, 21 June 2008 that is set for the initial time for the numerical simulation. The target cyclone of this study is marked by an arrow over the Arctic Ocean with its minimum pressure about 1,000 hPa. The red dashed line indicates the axis of trough with a strong baroclinicity, indicating the arctic front. Geographical names are listed in Fig. 4 for convenience.

The case 2012 appeared above the Central Siberian at 18Z 2 August 2012, and moved to the Arctic Ocean showing a development in the central pressure. The minimum pressure in the life cycle is 965 hPa. The value is a historical record for August Arctic cyclones. The case 2012w appeared at the northern edge of the Scandinavia peninsula, which became a pre-existing Arctic cyclone for the case 2012. From Simmonds et al. (2008) and Simmonds and Rudeva (2012), the Arctic cyclone with the minimum pressure below 980 hPa is very rare in summer, especially in August. Therefore, the Arctic cyclones in this study are fairly intense cases.

2.2 Interpolation

To track cyclone centers in a high resolution, we generated the Equal-Area Scalable Earth (EASE) grid system centered on the pole with horizontal grid of 20 km. Then, we interpolated the meteorological data of the EASE grid system from a latitude/longitude coordinate system using a bi-cubic spline interpolation. We tracked the cyclone centers on the sea level pressure field of the EASE grid system.

A cylindrical coordinate system is useful for analyzing the structure of cyclone such as the primary circulation, the secondary circulation and the thermal structures. We

converted the meteorological data from the latitude/longitude coordinate system into the cylindrical coordinate system around the cyclone center using the bi-cubic spline interpolation. Here, the north derection was derived from the cyclone centers and the North Pole, then the north is defined as the positive derection of y-axis in a Cartesian coordinate system. That direction was defined as a standard direction of the azimuth of the cylinderical coordinate system. The resolution of the cylindrical data is 10 km in a radial direction with 1 degree in deflection angle. Therefore, the positive derection of x-axis in the Cartesian coordinate or the cylinderical coordinate system indicates the east derection. Note that we decomposed zonal wind and meridional wind components on the latitude/longitude coordinate into tangential and radial wind components on the cylindrical coordinate. We defined a temperature deviation as a deviation from an environmental mean value. The value was averaged within 4000 km in diameter from the cyclone center. That is,

$$T^{'} = T - \int\int_{r=0}^{r=4000km} T dr d\lambda,$$

where $T^{'}$ is temperature deviation, r is radii from the cyclone center and λ is angle. We assumed that the environmental mean temperature does not change for the short time period such as one week. Therefore, we can investigate well the time development of warm core of the cyclone. Thus, we can measure the cyclone structure in more detail. To detect some representative structure of the cyclones, we calculated some azimuthally averaged fields of tangential, radial, vertical velocity, relative vorticity, potential vorticity and temperature deviation.

2.3 Simulation settings

The computation was carried out at the T2K-Tsukuba system in the Center for Computational Sciences of the University of Tsukuba. The horizontal resolution of the model is set at glevel-9 (approximately 14 km), and the vertical resolution is 40 layers of Lorenz grid from the surface up to 38 km. Although the resolution may be still coarse, this horizontal resolution allows us to use cloud microphysics instead of the cloud parameterization. A numerical simulation of the rapid development of the arctic cyclone is conducted using the following initial data. Initial atmospheric data for the NICAM are prepared by interpolating the objective analysis data of Japan Meteorological Agency/ Global Spectral Model (JMA/GSM) on 00Z, 21 June 2008 with a resolution of TL959L60, which has a horizontal resolution approximately of 20 km. Initial sea surface temperature and sea ice data for NICAM are obtained from GISST climate data released by the Hadley Center. Then, we intergrated for three weeks with basically 6 hourly output.

The cloud microphysics scheme is essential for our simulation, which is introduced in general for the resolution above glevel-9. In this study, we use the cloud microphysics scheme by Grabowski (1998) which is a simple microphysics for five classes of water (water vapor, cloud water, cloud ice, liquid water and snow). An improved version of Mellor and Yamada level 2.0 with moist closure model (Nakanishi and Niino 2004) is used for the boundary layer. The radiation scheme is MSTRNX. The simulation was performed without any assimilation technique.

2.4 Potential vorticity thinking

Thinking from potential vorticty (PV) perspective is important for the studies about cyclones. Hoskins et al. (1985) developed the concept of PV thinking in order to under-

standig atmospheric circulation from the large scale to synoptic scale and its interactions. Ertel potential vorticty by Ertel (1942), to define vortex intensity such as the dynamical tropopause used in this study, is given by

$$Q = \frac{1}{\rho}\boldsymbol{\omega}_a \cdot \boldsymbol{\nabla}\theta, \tag{1}$$

where ρ is density, $\boldsymbol{\omega}_a = \boldsymbol{\omega} + 2\boldsymbol{\Omega} = \boldsymbol{\nabla} \times \boldsymbol{U} + 2\boldsymbol{\Omega}$ is the absolute vorticity. $\boldsymbol{U} = (u, v, w)$ is the three dimentional velocity vector.

$$\boldsymbol{\nabla} = \left(\frac{\partial}{\partial x}, \frac{\partial}{\partial y}, \frac{\partial}{\partial z}\right)$$

is the gradient operator. Potential vorticity and the PV perspective are well summerized by Hoskins (2015). Potential temperature is defined by

$$\theta = T\left(\frac{p_0}{p}\right)^{R/C_p}, \tag{2}$$

where T is temperature, p is pressure, p_0 is 1000 hPa, R=287 $\mathrm{JK^{-1}kg^{-1}}$ is the dry air gas constant, and C_p=1004 $\mathrm{JK^{-1}kg^{-1}}$ is the specific heat capacity of dry air at constant pressure.

Vortex intensity changes can be quantified using Ertel potential vorticity equation:

$$\frac{\partial Q}{\partial t} = -u\frac{\partial Q}{\partial x} - v\frac{\partial Q}{\partial y} - w\frac{\partial Q}{\partial z} + \frac{\boldsymbol{\omega}_a}{\rho} \cdot \boldsymbol{\nabla}\frac{D\theta}{Dt} + \frac{D\theta}{\rho} \cdot \left(\boldsymbol{\nabla} \times \frac{\boldsymbol{F}}{\rho}\right), \tag{3}$$

or

$$\frac{DQ}{Dt} = \frac{\boldsymbol{\omega}_a}{\rho} \cdot \boldsymbol{\nabla}\frac{D\theta}{Dt} + \frac{D\theta}{\rho} \cdot \left(\boldsymbol{\nabla} \times \frac{\boldsymbol{F}}{\rho}\right). \tag{4}$$

This implys that vortex intensity change can only occur in the presence of diabatic or frictional process due to PV being a conserved quantity. But, this study focused on the adiabatic process, we took notice about the vertical advection term in pressure coordinate,

$$-\omega\frac{\partial Q}{\partial p}, \tag{5}$$

which plays an key role on the downward intrusion of tropopause. However, in discussion section, we discuss the vortex intensity change by radiational (diabatic) process and frictional process.

To examine the intensity of the vortex of the cyclone, due to output data is organized in pressure coordiante system, we calculated three-dimensional Ertel potential vorticity in the units of PVU (=10^{-6} m^2 s^{-1} kg^{-1} K) with pressure coordinates described by the following from,

$$Q = -g\left(\zeta + f\right)\frac{\partial\theta}{\partial p} - g\boldsymbol{k}\left(\frac{\partial \boldsymbol{V}}{\partial p} \times \boldsymbol{\nabla}_p\theta\right), \tag{6}$$

where ζ is vertical component of relative vorticity, f is a planetary vorticity g=9.81 ms^{-2} is a gravitational acceleration, θ is potential temperature, $\boldsymbol{V} = (u, v)$ is horiaontzal velocity vector, $\boldsymbol{k}$ is a unit vector of vertical component and $\boldsymbol{\nabla}_p$ is horizontal gradient operator on the pressure coordinate system.

2.5 Baroclinicity

Baroclinicity is the main role on the development of the mid-latitude cyclones. Therefore, to discuss the intensity of baroclinicity may be important. We defiend following formula as an intensity of baroclinicity,

$$\|\boldsymbol{\nabla}_p\theta_e\| = \sqrt{\left(\frac{\partial\theta_e}{\partial x}\right)^2 + \left(\frac{\partial\theta_e}{\partial y}\right)^2}, \tag{7}$$

where x is longitude, y is latitude and θ_e is equivalent potential temperature defined by

$$\theta_e = \theta\exp\left(\frac{L_c q_s}{C_p T_{LCL}}\right),$$

where L_c is the latent heat of condensation, q_s is the mass of wator vapor per unit mass of dry air in a saturated parcel and T_{LCL} is the temperature of the lifting condensation

level (LCL). Also vertical wind shear on the pressure coordinate system is defined by

$$\left\| \frac{\partial V}{\partial p} \right\| = \sqrt{\left(\frac{\partial u}{\partial p} \right)^2 + \left(\frac{\partial v}{\partial p} \right)^2}, \tag{8}$$

where $\boldsymbol{V} = (u, v)$ is horiaontzal velocity vector. In this study, the vertical wind shear is calculated between 400 hPa level and 850 hPa level.

2.6 Potential temperature budget

We calculated the semi-lagrange potential temperature budgets, to understand how the warm core develop, by following equation,

$$\frac{\delta \theta}{\delta t} = -\left(\boldsymbol{V} - \boldsymbol{c}\right) \cdot \boldsymbol{\nabla_p} \theta - \omega \frac{\partial \theta}{\partial p} + \frac{d\theta}{dt}, \tag{9}$$

where $\boldsymbol{V} = (u, v)$ is horizontal wind vector, $\boldsymbol{c}$ is moving vextor of cyclone system, $\boldsymbol{\nabla_p}$ is the horizontal gradient operator on pressure coordinate and $d\theta/dt$ is diabatic term. The diabatic term calculates as the residual. The system moving vectors are derived from the position of cyclone centers. Each terms were calculated by the areal mean in radius of 500 km from cyclone center on the EASE grid system, then they are integrated vertically by following forms,

$$A = \int_{P_1}^{P_2} \int_{r=0}^{r=500km} AdSd\ln P,$$

where A is the each term, P_1 and P_2 are the pressures at the optional heights. In this study, The potential temperature in two layers of upper 100-300 hPa and lower 300-925 hPa were measured by above method. Thus, we discuss how the storm relative upper warm core and lower cold core develop.

3 Performance of NICAM

To evaluate the performance of the simulation by NICAM, we compared the intensities and tracks of the simulated cyclone with the reanalysis data of JRA25/JCDAS. Figure 5a plots the minimum sea level pressure (MSLP) from the genesis of 10 June to 21 June of the initial date for NICAM. We show in Fig. 5b the three time series of MSLP (red) and minimum geopotential height (blue) at 500 hPa (MGPH500) of the simulation, and a time series of MSLP of the reanalysis data (black). The MSLP of the most deepened in the time series of simulation was about 971 hPa from 042 hr to 054 hr, and that of reanalysis was about 978 hPa at 030 hr. The weaker development in the reanalysis may partly be due to the coarser resolution. The decreasing rates of MSLP for simulation and reanalysis data were about 20 hPa over 24 hours from 018 hr to 042 hr and about 17 hPa for 24 hours from 006 hr to 030 hr, respectively. Thus, the simulation successfully reproduces the rapid development of the cyclone, though the transitions to mature and decaying phases occurred later, probably due to the spin-up time for dynamics and physics of the model. The MGPH500 of the simulated cyclone decreased steadily by 054 hr, and increased after 054 hr. The weakening of the cyclone at the sea level started at 054 hr, and the increasing trend of the MSLP is nearly constant. Therefore, the result suggests that the development of the cyclone at sea level was synchronized with the upper level. Figure 5c shows the cyclone tracks in the model (red line) and reanalysis (black line) and the location of MGPH500 in the model (blue line). The cyclone generated on 00Z, 10 June 2008 (Fig. 5c) at the boundary of the Laptev Sea, the East Siberian Sea and the Arctic Ocean (cross symbol), then it moved around the Arctic Ocean (gray line) from the cyclogenesis to cyclolysis. In the mature phase (Fig. 5b), the MSLP was less than 980 hPa. Since the cyclones over the Arctic Ocean showing less than 980 hPa are very rare in summer (Simmonds et al. 2008), this

is the case of sufficiently strong arctic cyclone. Both cyclones moved randomly, but the simulated cyclone moved longer than the reanalysis. In addition, the overall track of the simulated cyclone at sea level was similar to that at 500 hPa. The inset in Fig. 5c illustrates the distance between the centers for MSLP and MGPH500 in the model. We confirm that the distance is sufficiently small indicating the nearly barotropic structure, except for the time at 030 hr and 096 hr. Thus, the cyclone at the sea level was tightly connected with the cyclone at the upper level. Since the simulated Arctic cyclone was highly barotropic, we defined the center of Arctic cyclone as that at 500 hPa in this simulation as a working hypothesis, because we can track the cyclone center more smoothly at the 500 hPa level.

4 The structure of Arctic cyclones

4.1 Relationship between polar vortex and surface cyclone

Figure 6 (a), (b) and (c) show the relationship between the lower stratospheric cyclones (200 or 300 hPa) and the surface cyclones after 24 hours from the cyclones appeared for the case 2008, the case 2012w and the case 2012, respectively. And Fig. 6(d) indicates the same as (a)-(c), but for the mature stage of the case 2012. The surface cyclone for the case 2008 developed showing a larger scale of 2000 km in diameter directly below an axisymmetric upper polar vortex (Fig. 6a). The development directly relating to the polar vortex is a key phenomenon for the Arctic cyclone in early stage. The surface cyclone for the weaker smaller case appeared showing a smaller scale of 500 km in diameter below a lower stratospheric trough connecting to the center part of the polar vortex with a closed cyclone (Fig. 6b). This information indicates that the cyclonic perturbation was weaker than the stronger cases in the upper troposphere to the lower stratosphere. Besides, it implies that the smaller cyclone connects to some asymmetric components of the upper polar vortex which is able to form the Arctic cyclone. The surface cyclone associating with the center part of the upper polar vortex has a large scale compared to the cyclones appearing in the surrounding part, reflecting the scale of the polar vortex. The surface cyclone for the case 2012 appeared showing the baroclinic structure below a jet stream which is involved with a pre-existing Arctic cyclone (Fig. 6c). A trough extending to the center part of the polar vortex is seen at the northwest side of the surface cyclone. This pattern is similar to the mid-latitude cyclones in which the development is expected. Furthermore, at the northeast side of the baroclinic cyclone, there is another surface cyclone below the polar vortex organizing the typical Arctic cyclone. This pre-existing cyclone had originated as the smaller weaker

cyclone in Fig. 6(b), and it has become a greater cyclone gradually for 5 days by the time 18Z 3 August 2012. This initially weaker Arctic cyclone played an important role in the following development of the case 2012 cyclone. The baroclinic cyclone which is seen in Fig. 3(c) grew rapidly indicating the minimum sea level pressure in Fig.3 (c), and then the developing cyclone merged with the pre-existing Arctic cyclone organizing a typical Arctic cyclone. The mature stage of the case 2012 cyclone has a large horizontal scale of 3000 km in diameter showing the high symmetricity. Thus, and as mentioned above, the formation of the Arctic cyclone occurs in conjunction with a single upper polar vortex core.

4.2 Horizontal structure at the surface

Figure 7 illustrates the time-radius cross sections of azimuthal mean tangential wind, radial wind, temperature and specific humidity near the surface level for the case 2008. The range of values of the tangential wind is 6 to 12 m/s during a life cycle of the cyclone. The surface jet locates around 500 km in radius. The maximum tangential wind of 12 m/s was recorded just after when the cyclone recorded a minimum pressure in its life cycle. The cyclonic circulation prevails in a radius of 1500 km, which suggests the cyclone is a huge vortex of 3000 km in diameter. It is more than three times in size compared with the typical tropical cyclone. The radial wind is negative throughout a period. It means the air is inflowing toward the cyclone center from outside. The inflow region is 1500 km radius corresponding to the region of the cyclonic circulation. The maximum of the inflow is 4 m/s which was recorded when the cyclone was the matured stage.The surface temperature in a cyclonic vortex is approximately 0 ℃ in the life cycle in agreement with the observations. The specific humidity in the vortex is low in association with the surface temperature. The region with lower temperature

and humidity coincides with the region of the inflow cyclonic circulation.

Figure 8 illustrates the same as Fig. 7, but for the case 2012. The two cyclones were involved in the intensification of this cyclone. The cyclone merged with another pre-existing Arctic cyclone (Fig. 3c). The cyclonic tangential winds in the early stage are significantly weaker than the case 2008. The tangential wind is rapidly formed as the cyclone developed. The peak intensity of the tangential wind is the same as the case 2008. The region governed by the cyclonic circulation expands to more than 1500 km in radius. We can see the drastic structure change in the surface temperature field. The cyclone located over the continent had warm temperature and high moisture, but moved on the iced ocean with cold temperature and lower moisture. The temperature of the cyclone region when it locates on the ocean is nearly 0 ℃ as seen with the case 2008.

4.3 Vertical structure

It is important to understand the three dimensional stereoscopic structure for the theory of Arctic cyclones. From Fig. 7, we find that the structures of the cyclone have steady state during the life cycle. Therefore, we are able to extract the typical structure of the Arctic cyclone by time averaging.

Since tropopause folding is a common structure among cyclones, to analyze tropopause is important for the research of the cyclones. Figure 9 shows the lifetime mean potential vorticity (PVU, $10^{-6}\mathrm{m^2s^{-1}kg^{-1}K}$), geopotential height (m) at 250 hPa and 500 hPa, and sea level pressure (hPa) of the Arctic cyclone (case 2008). We find from Fig. 9 (a) that there is an isolated potential vorticity anomaly, associating with the intense upper polar vortex having symmetric circulation at lower stratosphere. This stratospheric vortex vertically binds the mid-tropospheric vortex tightly, indicating cyclonic potential vortic-

ity anomaly (Fig. 9b). The surface cyclone appears just below the upper polar vortex in the high potential vorticity region at 850 hPa (Fig. 9c). The horizontal scale of the cyclone is 1500 km in radius showing high symmetricity from lower to upper altitude.

Figure 10 illustrates the radius-height cross section of azimuthally averaged tangential wind, radial wind, vertical velocity, relative vorticity and temperature deviation from the environmental mean on 12Z 10 June for the case 2008, when the Arctic cyclone was in the appearing stage. And, figure 11 illustrates the same as Fig. 10, but on 06Z 22 June, when the Arctic cyclone was mature stage. Compare the structue in the appearing stage with in the mature stage, we can find that both the dynamical structure and thermal structure is similar. The snapshot figures during the life cycle show the same structures as the Fig. 9 and Fig. 10, although there are some fluctuations for the intensities of the secondary circulation in time.

Figure 12 illustrates the radius-height cross section of azimuthally averaged tangential wind, radial wind, vertical velocity, relative vorticity and temperature deviation from the environmental mean for the case 2008. The figures are time average during 00Z 10 June 2008 to 18Z 26 June 2008 (for 17 days). The upper jet locates at 300 hPa, radius of 400-1000 km, and its maximum is over 20 m/s. The cyclonic wind covers the whole length of graphic, exceeds a radius of 2500 km. This huge cyclonic circulation with the deep tropopause folding which descends down to 500 hPa from 300 hPa is related to the upper polar vortex. The Arctic cyclone is a wide-scale vortex of a deep cyclonic primary circulation from the surface up to the stratosphere.

There is a secondary circulation within the vortex of the cyclone. The outflow at the upper troposphere (200 -500 hPa) is seen in Fig. 12(b). In the boundary layer, it is an inflow (Fig. 12d). It shows updraft within the 1000 km radius, the region of peak intensity locates at 500 hPa level of a cyclone center. On the other hand, the figure shows

the downward current outside the 1000 km radius. Note that it shows a downdraft at the lower stratosphere (70-250 hPa) around the cyclone center.

The positive relative vorticity related to the deep cyclonic circulation stretches up to the stratosphere of 50 hPa level from the surface. The temperature deviation indicates a cold core in the troposphere and a warm core in the stratosphere as seen in Fig. 11(f). The center of the warm core locates at 300 hPa in agreement with the previous study by Tanaka et al. (2012).

The sustained downward airflows at the lower stratosphere are able to intensify the warm core by the adiabatic heating process. This effect has the potential to maintain the upper air and surface cyclones, causing the adiabatic cooling by the ascent flows in the troposphere through the boundary layer Ekman pumping. The value of the vertical motion is 0.6 mm/s at the lower stratosphere, which causes 0.53 K/day of adiabatic heating. The possible factors of the tropospheric cold core are adiabatic cooling and radiative cooling (Cavallo and Hakim 2010), as well as the appearing location where temperature is relatively low in comparison with surrounding regions.

Figures 13, 14 and 15 illustrate the same as Figure 10, but in the early developmental stage for the case 2012, in the appearing stage for the case 2012w and the mature stage for the case 2012, respectively. In the early stage (Fig. 13), the vortex shows clearly the baroclinic structure. We can find from the figure that the negative tangential wind or anti-cyclonic circulation at the upper troposphere and the shallow cyclonic circulation at the lower troposphere. The secondary circulation and the lower stratospheric downdraft are also seen in this case. The vorticity above the 500 hPa level is negative or shows an anti-cyclone. The cyclone was marked by a cold core at the lower stratosphere and a warm core at troposphere in that stage.

The pre-existing Arctic cyclone (case 2012w) indicates the sturucre of Arctic cy-

clone, for exampe, upper cyclonic jet of 8 m/s or lower stratospheric warm core, in the apperaring stage. There are two peaks in the vorticity distribution (Fig. 14e), one locates 200-500 hPa level indicating polar vortex, the other locates 600-1000 hPa level indicating the surface cyclone. This struxture is unique in case 2012w. Subsequently, however the case 2012w cyclone strenghened the structure of Arctic cyclone (not shown), the cyclone merged with the baroclinic cyclone(case 2012).

In the mature stage (Fig. 15), the cyclone had a structure of the typical Arctic cyclone, such as a deep cyclonic primary circulation with the large positive vorticity from the surface to the stratosphere, a shallow inflow layer, a warm core at the stratosphere and a cold core in the troposphere. This fact indicates the structure after the merging depends strongly on the pre-existing Arctic cyclone. The case 2012 is characterized by this structure change from the cold core to the warm core at the lower stratosphere, indicating a shift from the ordinary baroclinic cyclone to the typical Arctic cyclone. The following difference is found; the typical Arctic cyclones have a steady structure during the life cycle, on the other hand, the mid-latitude cyclones have a large structural change in the development. In the Arctic cyclone, the cyclonic vorticity near the surface is connected to the polar vortex in the stratosphere, whereas the cyclonic circulation is confined within the troposphere in the mid-latitude cyclone. The major difference between the mid-latitude cyclone in occluded stage and the Arctic cyclone is the existence of the persistent warm core in the stratosphere for the Arctic cyclone which is not maintained for a long time for the mid-latitude cyclone.

4.4 Summary and discussion

We conducted some analyses for the cases of the well-known Arctic cyclones using the cylindrical coordinate system. We investigated in this study the three dimensional

structure of the Arctic cyclones in detail.

Figure 16 shows the conceptual model of the vertical structure for the Arctic cyclones. The Arctic cyclone has a deep barotropic cyclonic circulation, a secondary circulation in the troposphere, a downdraft at the lower stratosphere, a coupling of a warm core at stratosphere and a cold core in the troposphere indicating a deep tropopause folding. These structures are similar to the cold vortices (Hoskins et al. 1985; Thorpe 1986; Wirth 1995) appearing as a cut-off low system in the mid-latitudes, and are different from the tropical cyclones and mid-latitude cyclones. The horizontal scale of the Arctic cyclone circulation reaches 5000 km in diameter at upper level, and is one of the largest cyclones which are found on the Earth. Some mid-latitude cyclones, especially "Bomb" cyclones (Sanders and Gyakum 1980) developing over the ocean, have same horizontal scale. For the Arctic cyclone, the positive relative vorticity related to the deep axisymmetric cyclonic circulation stretches up to the stratosphere of 50 hPa level from the surface indicating a connection with the stratospheric polar vortex. We could often find the cyclonic circulation on the weather analyses of vicinity of the tropopause (200-300 hPa) for the well-developed occluded cyclone (e.g., Morgan and Nielsen-Gammon 1998; Wang and Rogers 2001). But, the cyclonic circulation of the mid-latitude occluded cyclones disappears with height above the tropopause. Thus, the Arctic cyclone at the surface is characterized by the deep stratospheric polar vortex, which is a different from the occluded cyclone in terms of the vertical scale.

Tropopause polar vortices are often found on the tropopause in the Arctic. Cavallo and Hakim (2010) provided the structure of the tropopause polar cyclones. Compared with their results, though the basic structure of the Arctic cyclones is similar to the tropopause polar cyclone, the scale and the intensity of the Arctic cyclones are significantly larger than that. The major difference in the Arctic cyclone is found in the

vertical structure producing the surface cyclone while it is unclear in the tropopause polar vortex. It is found that the Arctic cyclone is characterized as one of the tropopause polar vortices, but it is connected with the polar vortex of all the stratosphere, and the cyclonic circulation reaches to the ground, generating a secondary circulation which produces the cold core in the troposphere by the updraft from the surface level. We find that the cyclone of the case 2008 was generated with some axisymmetric cyclonic winds at the surface level, while that of the case 2012 was not. This result implies the case 2008 cyclone was formed by the barotropic process, and the case 2012 cyclone was generated on the front with no cyclonic circulation. The case 2012 cyclone developed strongly under the influence of the tropopause polar cyclone (Simmonds and Rudeva 2012). The change of symmetric structure seen in this study represents that the cyclone was merged with the taller polar vortex. Thus, the cyclone became the structure of the typical Arctic cyclone.

Finally, this study could not show the generality. To make the generality, further studies are needed such as the statistical studies and the modeling studies or further analysis for the individual Arctic cyclones.

5 Development mechanism of the Arctic cyclones

5.1 Development of thermal structure of the Arctic cyclones

Figure 17 indicates the development of the lower stratospheric warm core and the tropospheric cold core for the both cases. In the case 2008, the lower stratospheric warm core maintains its intensity all the life cycle, which is uniqueness of the cyclone. The tropospheric cold core became gradually stronger as weakening of the cyclone by 18-19 June. In the case 2012, the lower stratosphere is the cold core region at the beginning stage. As the cyclone developed, the thermal structure changed dramatically. In the early stage of development, the troposphere gradually warmed to 4 August indicating weak warm core (Fig. 17b). The evolution of the case 2012 is similer to the life cycle model proposed by Shapiro and Keyser (1990). After then, the troposphere rapidly cooled indicating strong cold core. On the other hand, the lower stratosphere warmed rapidly indicating intense warm core. This dramatic change of thermal structure was in agreement with the merging event as mentioned above (Fig. 13-15).

5.1.1 The Arctic cyclone of the case 2008

Figure 18 shows the potential temperature tendency term, the horizontal advection term, the adiabatic term by vertical flows and the diabatic term (Eq. 9) for the case 2008. The diurnal change is commonly observed in all the life cycle , however, there is no conspicuous change in the potential temperature tendencies (Fig 18a). In lower stratosphere of 100 - 300 hPa level, the adiabatic term is positive all the life cycle (Fig. 18c), and which seems to be canceled by the adiabatic cooling (Fig. 18d). In the phase of intensification from 00Z, 19 to 06Z, 22 June, the horizontal advection term is positive indicating the warming from the lower stratosphere to the troposhere (Fig. 18b). From

Fig. 18, the adiabatic wariming and the horizontal advection are very important on the intensification and maintenance of the cyclone.

Figure 19 shows the how the upper warm core develop. Two warming period can be seen in the life cycle. One is the inital apperaring phase from 00Z, 10 to 00Z, 11 June, the other is the later rapid intensification phase from 18Z, 19 to 06Z, 22 June.

Table 1 indicates the layer averaged potential temperature budget between 100 and 300 hPa level. The layer mean potential temperature increases 3.3 K from 384.5 K to 387.8 K in the apperaring phase. The adiabatic effect by the vertical motion (downdraft) is the most important in the apperaing phase (see Fig. 19). The horizontal warm advection also plays a role in the intensification of the warm core. The diabatic term acts to weaken the warm core.

Table 2 indicates the same as Table 1, but in the later rapid intensification phase from 18Z, 19 to 06Z, 22 June. The layer mean potential temperature increases 3.0 K from 385.5 K to 388.5 K in this period. The adiabatic effect in this period is 3.6 K, which accounts for 119 % of the total warming. The horizontal advection is also positive contribution. The diabatic term is negative to weaken the warm core. Therefore, the diabatic term play as the counterpart to both the adiabatic warming and positive horizontal temperature advection. All the life cycle, the adiabatic warming playes a major role in the intensification and maintenance of the upper warm core structure of the Arctic cyclone.

Table 3 indicates the layer averaged potential temperature budget betwee lower 300 and 925 hPa level in the appearing phase. The layer mean temperature undergoes very little change, which is a remarkable feature. The contributon by the horizontal advection is vanishingly small. In lower layer of 300 - 925 hPa level, the diabatic effect have a postitive contribution, but which is canceled by the effect of the adiabatic cooling.

As a result, the layer mean temperature maintain to keep the cold core. Thus, the effect by the diabatic heating is relatively small due to the lower humidity. That is, in the beginning to early intensification phase, the development of the cyclone is controled by the mainly upper process, especially the dibatic warming by the lower stratospheric downdraft.

Table 4 indicates the layer averaged potential temperature budget between lower 300 and 925 hPa level in the weakening phase. The layer mean potential temperature decreases 3.5 K from 296.2 K to 292.7 K in this phase. From Fig. 18c, the adiabatic cooling controls below 500 hPa, which is the most important nature of the Arctic cyclone. But in the layer from 300 to 500 hPa, the adiabatic warming is often seen in the phase, which offsets the the lower adiabatic cooling in the mean temperature field. The diabatic effect is negative reflecting intensified tropopause radiative cooling around 400 hPa level (Fig. 18d). Thus, both the adiabatic cooling and radiative cooling contribute to make cold core below the tropopause in the weakening phase.

Table 5 shows the layer averaged potential temperature budget betwee lower 300 and 925 hPa level in the later rapid intensification phase from 18Z, 19 to 06Z, 22 June. The layer mean potential temperature increases 3.0 K from 295.0 K to 298.0 K in the phase. The warimng is controled by the horizontala advection, which is twice as large as the total wariming. While, the adiavatic effect has negative contribution to keep cold dore structure due to intensifed updraft by the rapid intensification. The diabatic effect is varnishingly small through the rapid intensification period. Thus, it is the small contrubution of the diabatic heating indicating condensation to develop the thermal structure averaged in troposphere. The contribution of the diabatic effect is temporal positive, and which is almost negative all the life cycle. This is a unique feature of the Arctic cyclone.

5.1.2 The Arctic cyclne of the case 2012

Figure 20 shows the same as Fig. 18, but for the case 2012. There is clear change in the potential temperature tendencies. From 12Z, 4 to 18Z, 6 August when the cyclone showed maximum intensity, the lower stratosphere warmed rapidly which was accounted by the horizontal advection term (Fig. 18b). This positive tendency is affected by the merging with the pre-existing Arctic cyclone. Note that the adiabatic term was positive all the life time just as same as the case 2008, which indicates that the adiabatic effect may play a main role on the maintenance of the Arctic cyclone (Fig. 18c).

Figure 21 shows the how the upper warm core develop. In contrast to the case 2008, a rapid change of the layer averaged potential temprature from 372 K to 391.3 K can be seen in Fig. 21. Table 6 indicates the layer averaged potential temperature budget between 100 and 300 hPa level from 00Z, 5 to 18Z, 7 August, when the cyclone is in the merging or maintenance phases. The layer averaged potential temperature increases 17.3 K in this period. The horizontal advection term becomes the most contribute factor, which accouts for 70 % of the total warming. Not only the horizontal advection with the merging event, but also the adiabatic warming play an importante role in the rapid intensification of the warm core of the Arctic cyclone. The adiabatic warming is larger than the diabatic cooling in the meriging and maintenace phases. The peak intensity of the adiabatic warming is 2.0 (K/6r) at 06Z, 6 August, when it is just after the merging event. The adiabatic wariming is twice times as large as the diabatic cooling in this period.

Table 7 shows the same as Table 6, but the layer averaged potential temperature budget between lower 300 and 925 hPa level. It decreases 13.3 K from 312.5 K to 299.2 K in this period. The adiabatic cooling by updraft is dominant in both phases, which accounts for 92 % of the total cooling. The horizontal advection has positive

contribution for the cooling. While, the diabatic effects act to warm slightly in the lower layer. Thus, the cold core transion is explained by the large adiabatic cooling and the moderate horizontal cold advection. The merging event completed in 24 to 48 hours in this case, from the analysis of the potenteal temperature budget.

5.1.3 The effects of the advections

Here, we consider the meaning of the temperature horizontal and vertical advections by axisymmetric flows. When the vortex indicates absolutely axisymmetric thermal structure, the horizontal temperature advection by the primary cyclonic circulation is little or none. The upper warm core of cyclone center is stretched by the secondary upper outward flows. This advection has an effect to warm up of the control volume of the cyclone.

The Arctic cyclone of case 2008 indicates large scale downdraft in the region of the cyclone center. The downdraft allows the heating the warm core indicating downward positive temperature advections. Thus, the secondary circulation forms and maintains the warm core by vertical and horizontal temperature advections. The feature of horizontal advections is that the additional heating is nearly zero without diabatic heating, that is, the warm anomaly moves only overlapping with the surface cyclone. A main reason of positive values of the horizontal advection is that the vortex has vertically asymmetric warm core. When the cyclone indicates asymmetric structures, the asymmetric components of the flows allow the cyclone region to warm up by the horizontal temperature advections, which is caused by the asymmetric flows such as the steering flow. Such advection may occur, when a cyclone merges with another or pre-existing cyclone. In particular, the warm up by the temperature advection may seem to be much stronger, when the mobile cyclone on the steering flow has the intense upper warm core.

5.2 The structure of Arctic cyclone and local front by NICAM

Figure 22 illustrates the horizontal maps of sea level pressure at 018 hr, 030 hr, 054 hr and 114 hr from the initial time simulated by NICAM. At 018 hr, the Arctic cyclone (hereafter, AC) is developing over the Arctic Ocean with the MSLP of 992 hPa (Fig. 22a). The horizontal scale of the AC is about a half of the Arctic Ocean. A mesoscale cyclone (hereafter, MC) with 998 hPa was generated around the AC near the boundary of the Eurasian Continent and the Laptev Sea. At 030 hr, the AC was developing gradually, showing the SLP of 988 hPa at the center (Fig. 22b). The MC had grown rapidly, and the pressure was as low as the AC. At 054 hr, the MC had merged with the AC, creating a single intense cyclone with 971 hPa (Fig. 22c). At 114 hr, the AC had weakened gradually and cyclone center at the sea surface was split into two parts (Fig. 22d).

We illustrate in Fig. 23 the air temperature (^{o}C) at 300 hPa, 500 hPa, potential vorticity (PVU) at 400 hPa and relative humidity (%) at 300 hPa at 024 hr. It was just before the rapid intensification (Fig. 5b), and the AC was nearly barotropic at that time (Fig. 5c). The AC in Fig. 23a has a warm core at 300 hPa (8600-9000 m), and its temperature is 15-20 ^{o}C higher than the surrounding regions. On the other hand, the AC in Fig. 23b indicates a cold core at 500 hPa. Thus, the AC changes the thermal structure between 300 and 500 hPa. Moreover, the temperature at 500 hPa is lower than that at 300 hPa around the cyclone center. Thus, the temperature distribution implies that the AC is similar to the cold-vortex or the cut-off low. The potential vorticity at 400 hPa in Fig. 23c shows the core exceeding the 2 PVU that corresponds to the dynamic tropopause. The high PV coincides with the upper level warm core. Thus, it implies that the tropopause has sunk into the core of the AC. This characteristic of PV is also in common with the cold-vortex. Since the warm core at 300 hPa is extremely dry (Fig.

23d) with relative humidity below 10 %, it suggests that the AC is a dry vortex with warm core in the lower stratosphere.

We illustrate in Fig. 24 the wind speed (m/s) at 300 hPa, vertical wind shear (m/s) obtained from Eqs. (8), the magnitude of front (K/10 km) at 850 hPa obtained from Eq. (7) and PV (PVU) at 850 hPa at 024 hr. In the southern side of the AC, there are many features of the baroclinicity. There is a strong jet from the East Siberian Sea to the edge of the Eurasian Continent. The jet is localized with its maximum wind speed greater than 50 (m/s) at 300 hPa (Fig. 24a). The northern half of the jet is associated with the large vertical wind shear (Fig. 24b). The intensity of vertical wind shear reaches 40 (m/s) over the East Siberian Sea. The intensities of the local jet and vertical wind shear are comparable to those of the mid-latitudes in winter. There is a front with a filament structure over the East Siberian Sea (Fig. 24c). The maximum magnitude of the front exceeds a level of 2.0 (K/ 10 km), and it is comparable to that of the mid-latitude cyclones. In addition, the front in Fig. 24c is coupled with a spiral band having high cyclonic and anti-cyclonic PV (Fig. 24d). It implies that the southern side of the front has a low level jet. Although the width of the spiral band of cyclonic PV is very narrow, the cyclonic PV is more than 2.0 PVU (Fig. 24d). The southern edge of the cold core is characterized by the enhanced baroclinicity with the southern warm air (Fig. 24b). The baroclinicity can enhance the MC by the local baroclinic instability along the front.

To achieve more understanding for three-dimensional structures of the AC and the front, we show in Fig. 25 the latitude-height cross sections of PV (PVU), zonal wind (m/s) and temperature deviation from its zonal mean (K) along the AB line in Fig. 24a. The AB line passes across the center of the AC and MC. There are two characteristic areas of high PV associated with the AC and the MC. The 2 PVU surface sinks toward

the 600 hPa level from 250 hPa in the AC center. The jet axis is located along 2 PVU surface. There is a high PV tower in the MC at 76^{o}N, and it extends from surface to 600 hPa. Therefore, the AC has the origin of high PV in the stratosphere, and the MC has that in the lower troposphere, indicating the PV generation by the diabatic heating.

The warm core is located at 300 hPa in the lower stratosphere. On the other hand, the cold core is located between 500 and 700 hPa in the troposphere. The intensities of warm and cold cores are 14 and -8 K, respectively. The center of AC is located just below a couple of warm and cold cores. The baroclinicity located at the south side of the AC is enhanced by the effect of the cold core. The axis of the cold core tilts toward the north with the height. The front also tilts toward the north with height. Thus, the cold core of the AC plays a role in the enhancement of the baroclinicity in the low level (Fig. 25b). The thermal contrast in the lower atmosphere which basically exists between the ocean and the continent may also contribute to the baroclinicity. Therefore, the front is strengthened by the combination of these two mechanisms.

5.3 The development of the Arctic cyclone in NICAM

To analyze the intensification of the AC, we calculated the time series of the vertical sections averaged within a 100 km radius from the center of AC. Since the cyclone has the warm core in vertical section, we calculated the amount of change of potential temperature from a reference state defined by the following equation:

$$\theta^{'}(p,t) = \int_{r=0}^{r=100km} \theta(x,y,p,t)dxdy - \theta_0(p) \tag{10}$$

where $\theta^{'}$ is the time change of the regionally averaged potential temperature. The first and second terms of the right hand side of Eq. (10) indicate the regionally averaged

potential temperature and the reference state. We calculated $\theta_0(p)$ as follows:

$$\theta_0(p) = \int_{r=0}^{r=100km} \theta(x, y, p, t_0) dxdy \tag{11}$$

where t_0 is a time of the first output. We show in Fig. 26 the time change of the regionally averaged potential temperature (K), vertical velocity (cm/s) and potential vorticity (PVU) by the time-height cross section.

5.3.1 The evolution of warm core

We argued in Sect. 5.2 that the AC has a warm core above 400 hPa and a cold core below 500 hPa. As time progresses until 036 hr, the warm core at the lower stratosphere appears gradually and the maximum change of potential temperature becomes 3 K. On the other hand, the cold core in the troposphere below 500 hPa becomes cooler in this period (Fig. 23a). It suggests that the warm core at 024 hr in Fig. 23b has enhanced by this time. The warm core in the lower stratosphere is sustained until 108 hr.

A drastic change in thermal structure appears at 042 hr. The cooling trend below 500 hPa changes to warming trend when the MC merges with the AC at the sea level. But after 042 hr, it becomes cooler gradually until 108 hr. The significant warming at 042 hr plays an important role for the rapid intensification of the AC. It supports the rapid pressure decrease at the sea level. Just before the AC to split off at 108 hr, the cold core in the lower troposphere is most prominent.

5.3.2 The role of vertical velocity

In this subsection, we examine the enhancement of the warm core. The lower stratosphere is extremely dry. The diabatic heating by the condensation of water vapor is negligibly small. We examine the enhancement of the warm core by the adiabatic

heating due to the descending dry air. In Fig. 26b, the layer from 200 to 400 hPa, which corresponds to the warm core, indicates downdraft until 030 hr. The intensity of the downdrafts is about 0.2 - 0.8 cm/s. If a parcel is in the downdraft with 0.5 cm/s, it descends 540 m in 30 hours. If temperature in the environment does not change vertically in that region, there is the temperature rise with 5 - 6 K by adiabatic process.

The sign of vertical velocity of the layer reverses at 060 hr, and the layer changes to updraft until 096 hr. The trend of MGPH500 (Fig. 5b) reverses to the increase in agreement with the change of sign of vertical velocity. It is a key signal for the decay process of the AC. There are some evidences for the formation of warm core by the downdrafts. We infer that the enhancement of the warm core due to the downdraft is strongly related to the intensification of the AC.

5.3.3 Vortex coupling and merging

The origin of the AC is seen in the upper level vortex, and that of the MC is seen in the lower level vortex. These vortices merge with each other in agreement with the rapid intensification of the AC. We present in this subsection the features of the PV in that period. The 2 PVU surface locates at 600 hPa throughout the time. The tropopause locally falls down to 600 hPa around the AC (Fig. 26c). A notable event occurs in the PV at 042 hr showing the sudden expansion of the high PV with 1.0 PVU down to the lower troposphere. By this event, the AC becomes a high PV for the entire troposphere. This event corresponds to the merging of two systems of the AC and the MC in the vertical direction. Therefore, the result suggests that the vortex coupling is an important mechanism for the rapid intensification of the AC.

When the tropopause expands down to 600 hPa by the AC, the tower also expands up to 600 hPa that results in the vertical merging of the PV. We show in Fig. 27 the

horizontal plots of PV at 600 hPa in the rapid intensification phase. There are multiple mesovortices with high PV around the core of the AC in the form of local fronts at 024 hr (Fig. 27a). The clear local fronts construct the spiral band of PV. The mesovortices associated with the lower fronts are about to connect with the upper polar vortex (Fig. 25a). Note that the mesovortices at 600 hPa have merged into a single vortex at 048 hr, then the core of vortex becomes axisymmetric at 060 hr. These processes are similar to the merging and the axisymmetrization of the vortex in the tropical cyclones.

The cyclonic PV of the AC extended down to 600 hPa, and that of the MC is concentrated in the lower troposphere below 600 hPa. Therefore, the vertical advections of the PV at the 600 hPa are analyzed by evaluating the PV tendency (Eq. 5).

We show in Fig. 28 the vertical advection of PV and vertical velocity at 600 hPa for 030 hr, 042 hr and 060 hr. First two steps are in the rapid intensification phase, and a last step is at the mature phase. In the rapid intensification phase, the generation of PV by the vertical advection is active at red regions in Fig. 28a. One is seen at the back side of the AC, and the other is seen at the spiral bands of the MC. The region with PV generation at the back side of the AC corresponds to the downdrafts (Fig. 28b); on the other hand, that of the spiral band corresponds to the updrafts (Fig. 28b). Thus, there are two mechanisms for the PV generation by the vertical advection. In the mature phase (Fig. 28e), the vertical advection is weak in comparison with that in the intensification phase. Therefore, we confirm that the vertical advection is responsible for the rapid arctic cyclogenesis.

5.4 Baroclinic growth

In this section, we illustrate how the MC is intensified. Since the MC develops along the local front, it is necessary to examine the baroclinic growth. Figure 29 illustrates

the horizontal plots of relative humidity at 500 hPa, air temperature at 925 hPa, and the intensity of the front at 850 hPa for 030 hr, 048 hr and 066 hr. In this section, we illustrate how the MC is intensified. The times are in the rapid intensification, the mature and the decaying phases of the AC.

Figure 29a shows that the air near the center of AC is relatively dry at 500 hPa. However, there are some moist air-masses at 030 hr. One is located at the northern side of the center of AC with a round shape, and the other is distributed at the southern side with the shapes of spiral band. The former is accompanied with the AC, and the latter is accompanied with the MC. These systems mutually merge at 048 hr, and the AC becomes the well-developed spiral structure, which looks like the occluded cyclones in mid-latitudes. Thus, the rapid development of the AC is supported by the baroclinic growth of the MC. An extremely dry air-mass with the relative humidity of 10 % penetrates into the center of the AC along the spiral band (Fig. 29d), indicating dry intrusion (e.g., Browning 1998). In addition, a relatively warm air appears at the center of AC with its temperature 2.4 K higher than the surrounding regions at 925 hPa (Fig. 29e). As the AC develops, the local fronts are winded up in a spiral configuration (Fig. 29f). The convolution of a couple of dry and moist bands becomes more conspicuous at 066 hr, showing double spiral bands around the center of AC (Fig. 29g). This pattern looks similar to the cold core vortex seen in the mid-latitude, but the cold core reaches to the surface of the Arctic Ocean (Fig. 29h). The magnitude of the local front located at the edge of the Eurasian continent remains strong (Fig. 29c, f, i). It means that the thermal contrast between the ocean and land is robust. We expect an active meso-cyclogenesis along this Arctic frontal zone.

5.5 Concluding Remarks

In this study, we conducted a numerical simulation of a typical cyclogenesis in the Arctic in June 2008, using a cloud resolving global model NICAM with 14 km horizontal resolution, and investigated the structures and the intensification of the cyclone system. There are two characteristic structures in the cyclone system in the Arctic. One is a barotropic cyclone with a warm core in the stratosphere and a cold core in the troposphere, which is called the ‘ Arctic cyclone (AC)’. The other is a meso-scale baroclinic cyclone growing along the Arctic front, which is called the ‘ Mesoscale cyclone (MC) ’.

The AC is a dry vortex accompanied with a upper air polar vortex and a deeply depressed tropopause. The AC has some features in common with the cold core vortex in mid-latitudes, but the cold core reaches to the surface of the Arctic Ocean. Therefore, it is found that the AC is a kind of cold core vortex in the troposphere, with a warm core in the lower stratosphere. The AC is maintained by adiabatic heating by the downdraft in the lower stratosphere.

On the other hand, the MC is baroclinically developed along the local Arctic front, which is located at the boundary between the ocean and the continent extending from the East Siberian Sea. Many previous studies (e.g., Serreze et al. 2001; Inoue and Hori 2011) showed that the cyclones in the arctic region indicate baroclinic growth. The growth of the MC is consistent with the previous studies. Two mechanisms for the enhancement of baroclinicity are proposed in this study. The first is the heat contrast between the ocean and the continent as noted by the previous studies. The second is the effect of the cold core of the AC itself.

The rapid intensification of the AC simulated by NICAM is explained by the superposition of the development of the upper air polar vortex and the baroclinic growth of the MC in the lower troposphere. The AC is maintained by the merging with the

developing MC. The vortex of the AC is found in the upper level, and that of the MC is in the lower level. The vortex coupling by the vertical merging of the AC and MC is a major finding in this study. There are two notable processes for the intensification and the maintenance of the AC. One is a merging of the mesovortices with the vortex core of the AC. The other is an axisymmetrization of a vortex core after the vortex merging. Those vortex mergings are frequently found in the developing tropical cyclones. In this regard, the AC is similar to the tropical cyclones. The high PV is supported by the vertical advections of PV associated with the downdraft by the AC and the updraft by the MC.

This study analyzed only one case of the Arctic cyclone by the numerical simulation. Therefore, further studies are necessary for many cases to understand the Arctic cyclogenesis.

6 Discussion

6.1 Arctic cyclogenesis

Arctic cyclogenesis is different from traditional cyclogenesis which had been investigated in previous studies. The cyclogenesis is, for the extratropical cyclones, for the meso cyclones on the fronts, nothing else that a perturbation by the instability develops indicating the cyclones. While, the Arctic cyclone is a mean field cyclone derived from the upper polar vortex and is not caused by any instabilities.

Robust upper warm anomaly is responsible for the surface cyclone, in this study. What is the factor of the warm anomaly? It is considered both the adiabatic heating by downdraft and the radiative hating. Since the radiation effects act to make cold anomaly from Cavallo and Haim (2009, 2010) and this study, the radiative heating is negligible.

Lapse rate of temperature in lower stratosphere is almost constant or rather the temperature at upper level is high. It assumes that the temperature is constant, when an air descends into 1000 m below, the temperature of the air gets warm of 10 ℃. This study indicates that a downdraft of 0.6 mm/s in lifetime average governs in the lower stratosphere above the surface cyclone which indicates the temperature increase of 5 ℃ per 10 days (Fig. 11). The intensity of the temperature increasing rate is enough to grow up constantly and maintenance of the cyclone. Note that the importance of the adiabatic warming by the downdrafts is cleared in this study. The Arctic cyclonegesis occurs when the upper polar vortex accompanied with a warm core intensifies due to the adiabatic warming by downdraft.

The descending flow in the lower stratosphere which is part of the secondary circulation is driven by the forcing, such as the latent heating, radiative cooling or convergence of the momentum fluxes. Thus, some mechanisms are needed to intensify the downdraft

in the lower stratosphere. For example, the radiative cooling in the lower stratosphere or condensational heating in the troposphere are possible mechanisms. The diabatic cooling in the lower stratosphere drives the tropospheric secondary circulation with the outward flows, which could create the compensational downdraft in the lower stratosphere. Cavallo and Hakim (2010) and this study indicate the continuous diabatic cooling, that is, radiative cooling above the tropopause. Both mechanisms can be seen in Fig. 18 and Fig. 20. The positive contributions of the diabatic term in the stratosphere and negative contributions above the tropopause are counterparts of the positive contributions of the adiabatic term in the stratosphere and near the tropopause. Thus the downdraft in the stratosphere is intensified by the both diabatic effects. The positive diabatic effects could play another role on the intensification of surface cyclones. Thus, both the intensified downdraft in the lower stratosphere and the diabatic heating in the troposphere could contribute to the rapid Arctic cyclongenesis in the short period.

The diabatic heating by condensation is effective in the intensification of the traditional extratropical cyclone. However, due to the specific humidity is considerably less in the Arctic than the mid-latitude, the diabatic effects are largely offset by the adabatic cooling by updraft or the horizontal cold air advection. Therefore, the effects of diabatic heating are limited in the Arctic. Especially, in the weakening phase of the Arctic cyclone, the adiabatic cooling by the updraft could play a major role on the weakening due to the static stability becomes larger by the cooling.

As well as in a mag cup a rotation stops at final stage, the cyclonic circulation in the real atmosphere spins down by friction of the boundary layer and stops at last in few days. But, the Arctic cyclones have much longer lifespan. This study suggests that the continued warming by the downdraft in the lower stratosphere could offset a barotropic spin down for the Arctic cyclones.

It is considered that the part of the descended mass from the lower stratosphere is transported to the outside of the vortex at last by the accompanied outward flow in the lower stratosphere to upper stratosphere (Fig. 12) in the long time scale. But, in the timespan of Arctic cyclones, this mechanism is limited due to the secondary circulation, especially lower stratospheric downdraft, is relatively weaker.

6.2 The conditon of Arctic cyclogenesis

Is the Arctic favorable condition for the surface cyclone? At upper level the cyclone tends to have longer lifetime due to isolation from the jet stream. When the static stability is higher than the usual, the upper cyclone is hard to reach the surface. Strong cold anomaly in lower troposphere indicating higher static stability acts to cause the upper cyclone to disappear at the surface. The Arctic, especially the Arctic Ocean, is lower temperature region. Essentially, the surface cyclone is hard to from in the Arctic.

The topography has some effect on the upper level induced circulation by the larger surface drag, which can reduce a barotropic circulation near the surface. At the area of large roughness like mountainous topography the circulation becomes weak. The Arctic has a relatively lack undulation due to covered sea ice. The surface drag in the Arctic is weaker than the surrounding area because of the relative lack of land area and topography. Thus, view from this perspective, the Arctic is a region where the surface cyclone induced by the upper cyclone tends to occur. And topography, such as Iceland or Greenland, which causes lee-side cyclogenesis as the Arctic cycloenesis.

When the static stability weakens by some kind of factor, for example large scale condensational heating and radiative heating, the Arctic becomes a favorable condition for barotropically induced surface cyclone. Seen from seasonality, the summer is lower static stability than the other seasons, therefore the cyclone tends to live longer and

generate more in summer. Zhang et al. (2004) indicate this fact by statistical study.

6.3 Instability and Arctic cyclone

The instability does not contribute directly to development and maintenance of the cyclone, but an instability appearing on the Arctic front can contribute indirectly to that. When the meso perturbation appearing on the Arctic front develops, it has great influence in the development and maintenance of the Arctic cyclone merging with the parent Arctic cyclone. This assumption that the upper vortex indicating the Arctic cyclone propagates over the Arctic front, then vertical coupling occurs.

Some studies suggest the theory of coupling development in the mid-latitude. The theory proceeds according to following physical processes. It is experimentally known that when an upper cold vortex causes a coupling with a lower cyclone on the front, the lower cyclone develops rapidly for a short time.

Frontal studies of Arctic cyclones by LeDrew (1985) showed that the Arctic cyclone originated from the Arctic front. Inoue and Hori (2011) showed the Arctic cyclogenesis appearing on the marginal ice zone. In the Arctic, it is well known that there is a steep temperature gradient i.e. baroclinicity between the continent and the iced ocean in the lower troposphere.

Bjerknes and Solberg (1922) also indicated the theory of cyclone family. Viewing from this theory, the Arctic cyclone becomes a parent cyclone. In the surrounding region of the parent Arctic cyclone, it is thought to form various secondary cyclones, originated from such as arctic front waves, Iceland-Greenland mountain leeside waves and internal trough in cold air-mass.

6.4 Potential vorticity perspetive

6.4.1 The condition over the Arctic

The Arctic higher than 70 °N has a symmetric cold anomaly due to the iced Arctic Ocean, although there are some asymmetries such as the Greenland or Canadian Archiperago. From potential vorticity perspective, the near surface cyclonic circulation induced by the upper potential vorticity is decreased by the anti-cyclonic circulation induced by the near surface cold anomaly. Therefore, the cyclonic circulation can not usually see at weather maps in the Arctic of surface analysis.

6.4.2 Vertical Scale

Here, we discuss the vertical scale of the Arctic cyclone. The vertical scale of vortex induced by the upper potential vorticity (PV) anomaly is estimated on the basis of PV thinking (e.g., Hoskins et al. 1985) by following relational expression,

$$H = \frac{fL}{N}, \tag{12}$$

where H is the vertical scale (m) which is referred to as Rossby height, f is the planetary vorticity, L is the horizontal scale of upper PV anomaly, and

$$N^2 = \frac{g}{\theta}\frac{\partial \theta}{\partial z}$$

is a parameter of static stability (s^{-2}), where $g = 9.81$ (ms^{-2}) is the gravitational acceleration and θ is potential temperature. The PV amomaly of the Arctic cyclone of the case 2008 is about 2000 km at height level of 10000 m (Fig. 9a). When θ and $\partial\theta/\partial z$ presume 290 K and 1 K/100 m, then N is about 1.8×10^{-2} s^{-1}. And f presumes the value of the North Pole, then H is approximately 16000 m. Thus, the PV anomaly of the Arctic cyclone is a sufficiently large scale to stretch the surface. The fact indicates that

the scale of upper polar vortex is very important factor to the surface Arctic cyclones in the condition of higher static stability in the Arctic. And it suggests that the horizontal scale of upper polar vortex indicating the PV anomaly is required at least 1200-1500 km at 250 hPa (10000 m) level to create the Arctic cyclone.

6.4.3 Vertical coupling

The upper level cyclone has usually higher PV indicating the PV anomaly. On the coupling development in mid-latitudes, horizontal advection of PV may play an important role at higher levels. The PV intensification by the adiabatic processes by advection is more important than the diabatic heating in such cases.

Downward advection by vertical motion can intensify the PV from lower stratosphere to mid-troposphere. This study shows the merger of the upper downward PV advections and the lower upward PV advections is primary role on the rapid intensification (Fig. 28).

6.4.4 Longer durability

Blocking anti-cyclones are phenomenon having persistency in the mid-latitudes. From the PV perspective, the blocking is an isolated uncommunicative vortex having lower potential vorticity. Due to its uncommunicativity, the high potential vorticity does not advect from outside. There is no change of PV by latent heats inside the vortex.

Precipitation indicating diabatic heating is unfavorable of the durability of Arctic cyclones due to the downward gradient of the diabatic heating weakens upper PV. Therefore, for the durability of the upper cyclone, it is preferable that there is no precipitation. On the other hand, precipitation tends to create potential vorticity in lower atmosphere, and that acts to strengthen the lower cyclonic circulation (Stoelinga, 1996).

Thus, the PV tendency by diabatic heating has two-faced affection.

Wirth (1995) showed that a strong tropospheric diabatic heating of +10 K/day in the middle troposphere lead to the decay of the upper level cyclone within a few days. The cloud microphysics and vertical cloud extent indicate there being strong differential heating across the vertical extent of the cloud layer, with heating at the cloud base and cooling the cloud top.

In the Arctic cyclones with substantially longer lifetime, it is suggest that either the latent heating must be considerably weaker, or else there are other processes. This study indicates that there is some degree of diabatic heating in the middle troposphere for the case 2012. But vortex intensity near the tropopause does not change considerably, therefore the effects of cloud may be limited.

6.4.5 Radiative effects

In the lower stratosphere, both ozone and water vapor are main radiative effects. Water vapor causes lower stratospheric region to cool in the longwave, due to the small optical depth above the tropopause. Can the absorption of the short wave by ozone raise temperature at the lower stratosphere in the cyclone core? About the atmospheric general circulation, temperature distributions in the stratosphere are characterized by a radiative heating by ozone. Cavallo and Hakim (2010) revealed that the radiative heating rate of the core of cyclonic tropopause polar vortices is negative, especially its rate near the tropopause.

Randel et al. (2007) cleared that ozone acts to warm above the tropopause, while water vapor acts to cool the near tropopause. Hence, the vertical gradients of temperature enhanced near the tropopause. Relatively lower humidity above the vortex core is favorable condition to the maintenance of the warm core structure.

Cavallo and Hakim (2009) revealed that cloud top radiative cooling is the primary diabatic mechanism that intensifies the Tropopause Polar Vortices (TPVs) during the growth phase. Increasing amount of moisture in the vortex core, allowing the destruction of potential vorticity near the tropopause due to latent heat release to became comparable to the radiational positive PV tendency.

The Arctic is covered by lower thin clouds (Curry et al. 1996). From potential vorticity tendency, latent heat release in lower clouds creates high potential vorticity in boundary layer and in lower free atmosphere just above the boundary layer. It implies from potential vorticity perspective that the lower troposphere is lower static stability, which tends to stretch cyclonic circulation down to lowermost troposphere. Thus, cloud activity in the Arctic could relate to the Arctic cyclogenesis. But well organized Arctic cyclone has a cold dome in core region with higher static stability through the troposphere due to adiabatic cooling by secondary circulation. Therefore, in the maintenance of the structure, there may not be any diabatic effect by the latent heat release.

7 Conclusion

This study is a first detail investigation about the Arctic cyclones using the cylindrical coordinate system and the cloud-resolving numerical simulation by NICAM. In this study, we indicate that the Arctic cyclone is a unique cyclone originated in the Arctic, and which is different from any other cyclones. The structure, development mechanism, lifecycle and environmental conditions on appearing are particular for the Arctic cyclones. The characteristics of structure and development mechanism are described above in Sect.4.4 and Sect.5.5. Therefore, in this section, we summarize the characteristics of life cycle, environmental condition and other concluding remarks.

The one of the uniqueness of the Arctic cyclones is longer lasting than any other cyclones. This study proposes how the Arctic cyclone can be long lasting. Fig. 30 illustrates the schematic diagram of the Arctic cyclone life cycle. The thermal structure of the Arctic cyclone is very stable having an upper warm core and a lower cold core. This thermal stability is one of the factors to long lasting for the Arctic cyclones. Here, we explain the further reason. The life cycle of the Arctic cyclone is able to classify in following five phases. A first stage of the Arctic cyclone is indicated in Fig. 30a that the upper polar vortex accompanied with a warm core intensifies due to the adiabatic warming by downdraft or static stability in the troposphere weakens by some mechanism, which produces the surface cyclone. A second stae is indicated in Fig. 30b that as the adiabatic warming intensifies, the surface cyclone develops indicating strong low pressure. A third stage in Fig. 30c is that as the surface cyclone intensifies, the updraft in the troposphere becomes gradually dominant indicating cold core intensifying, which decreases the surface pressure of the cyclone. It suggests that the typical Arctic cyclone spends its life cycle in a state indicating the first to third stage.

Some Arctic cyclones transition into next phase indicating Fig. 30d. It shows

fourth stage of the life cycle that the cyclone often merges with other frontal cyclone originated in the Arctic front or the mid-latitudes, indicating more intensification of the pre-existing Arctic cyclone. The structures after merging inherit the structures of the Arctic cyclones. The final stage in Fig. 30e is that the lower stratospheric downdraft and the tropospheric updraft are balanced each other, indicating the surface cyclone maintains long time. Therefore, the Arctic cyclone can have long time scale about life cycle. If (b) and (d) occur simultaneously, the Arctic cyclone can be stronger than other Arctic cyclones, such as the case August 2012 recorded 964 hPa, which is the August record. Thus, the life cycle of the Arctic cyclone is unique, and which is different from the life cycle of the mid-latitude cyclones, proposed by Bjerknes and Solberg (1922), Hoskins et al (1985) and Shapiro and Keyser (1990). Note that the latent heat by condensation has only a small impact on the process of the Arctic cyclone due to very low humidity.

However, the continuances of each phase vary in accordance with the individual cases, the phase of intensification showing Fig. 30b lasts for 1 to 4 days. And the phase of dissipation indicating Fig. 30c and Fig. 30e last for more than 4 days in the cases of this study. Since the Arctic cyclone is upper level cyclone stretching the surface, the updraft acts to decrease the cyclonic circulation of the vortex. The longer time scale for the dissipation is thought to be due to the weaker updraft than other cyclones. The maximum mean updraft near the cyclone center is less than 1 cm/s (Fig. 12c), which is less than tenth part of the typical mid-latitude cyclones and hundredth part of the typical tropical cyclones. The merging phase is 1-2 days in the case of this study, but it is a good guess that the differences among individual cycolones are quite larger. The shortest case may be several hours, and the longest case may be more than 2 or 3 days.

It is difficult to identify the trigger of cyclone appearing due to the complicated

processes before the appearing, which is not usually able to on the analysis field such as the reanalysis data. The genesis process of the tropical cyclones has still been unsolved problem, although a lot of study had been conducted. The various processes are considered as the trigger of genesis of the tropical cyclones, including upper level divergence or lower level stretching. Therefore, it is difficult to study about the appearing process of cyclone. The trigger of intensified lower stratospheric downdraft forming the Arctic cyclone in the appearing phase (Fig. 30a) is also unclear problem at least in this study. As well as the tropical cyclone, for example, it is considered the local divergence in the lower stratosphere near the tropopause or the local convergence in the stratosphere as the trigger of the downdraft in the appearing phase. To clear the process of appearing of the Arctic cyclone may be important problem in the future works.

Environmental conditions on appearing are quite different between the Arctic cyclones and the mid-latitude cyclone. The mid-latitude cyclones appears under the polar jet and the subtropical jet indicating the large temperature gradient i.e. baroclinicity. On the other hand, the Arctic cyclone develops under a polar vortex which forms the atmospheric general circulation on the Earth. It is known that a barotropic cyclone is seen in the averaged sea level pressure field in the summer of stronger polar vortex. This fact implies that the Arctic cyclone is related to the upper polar vortex. Generally, the static stability is higher in the Arctic than the mid-latitudes. Threfore, the horizontal scale of the polar vortex is a key factor to the Arctic cyclogenesis.

This study investigated the relationship between the Arctic cyclone and the upper polar vortex using individual cyclones in the case 2008, 2012 and 2012w. The case of 2008 is a barotropic cyclone from the beginning indicating strong connection to the upper polar vortex. The relationship is peculiarity in the Arctic cyclone, and is not reported in any other previous studies about the mid-latitude cyclones. The relationship

between the polar vortex and the Arctic cyclone is not seen in the mid-latitude cyclones. The mid-latitude cyclones begin as the small perturbation by baroclinic instabilities. In the developing stage, an axis of cyclone center i.e. a trough axis indicates westward tilt, which means that the surface cyclone is not directly related to the upper polar vortex. But final form of the well-developed mid-latitude cyclones are similar to the Arctic cyclone due to the trough axis becomes verticality. It is not that the mid-latitude cyclones are a part of the polar vortex.

Both the Arctic cyclones and the mid-latitude cyclones have downward flows in their systems. The roles of the downdrafts are considerably different. The Arctic cyclones have the large scale continued downdraft in the lower stratosphere of 100-300 level despite weaker intensity. Such downdraft plays an important role on the intensification and the maintenance of cyclone structure. The continued downdraft causes the adiabatic heating, which is responsible for the intensification and maintenance of the lower stratospheric warm core compensating the radiative cooling. The lower stratospheric downdraft is one of the most remarkable natures of the Arctic cyclones.

As the mid-latitude cyclones develop, the downdraft is formed at the back side of the cyclone. The downdraft of the mid-latitude cyclones makes downward intrusion of the tropopause called tropopause folding. We are able to see this downward intrusion as the dry slot in the satellite imaginary. The mixing between the stratospheric air and the tropospheric air is mainly caused by the tropopause folding events. The tropopause foldings often are observed above not only at the fronts of mid-latutude cyclones but also at the polar fronts, the Arctic fronts and the upper level fronts.

The tropopause folding nature of the Arctic cyclones are also important. The location and scale of the tropopause folding of the Arctic cyclone is considerably larger than that of the mid-latitude cyclone and the cold cut-off cyclone. The folding down

to 500 hPa level locates at the cyclone center with horizontal scale of 1000 km. The large scale of tropopause folding relates to the upper polar vortex indicating the Arcic jet. The tropopause folding indicates that the core region of the Arctic cyclones may be important as an active area of the stratosphere-troposphere mixing.

To accumulate the investigation of an individual cyclone is fairly important for the understandings of the cyclone. This policy puts special emphasis on the individual character of a cyclone. To give generality for the Arctic cyclone, further statistical and numerical studies will be needed, but new perspectives of the structure and development mechanisms including life cycle for the Arctic cyclone are indicated in this study. As was mentioned at the beginning, cyclones have diversity. Since the cyclones can think of about many kinds, further studies about individual cyclone are needed to better understanding about the cyclone.

Ackowlegement

First of all, I would like to express special appreciation to Prof. Hiroshi L. Tanaka, Center for Computational Sciences, University of Tsukuba, for his variable comments and encouragements. This study was mostly supported by the GRENE Arctic Climate Change Research Project. I am thankful to Profs. H. Ueda, K. Ueno, H. Kusaka, M. Matsueda and Y. Kamae for their variable comments and suggestions. I am also thankful to Y. Wakazuki in Ibaraki University, T. Kato and M. Ishii in Meteorological Research Institute. I am most grateful to Prof. Masaki Satoh, Atmosphere and Ocean Research Institute, University of Tokyo, for various support on my numerical simulation by NICAM. I am grateful to all other students and staff of the Climatology and Meteorology Group, the University of Tsukuba, for their comments and supports. Finally, I am most thankful to my family for their support and understanding, especially to Yuki Aizawa for the graphic design of Fig. 16 and Fig. 30.

REFERENCES

Aizawa, T., H. L. Tanaka, and M. Satoh, 2014: Rapid development of arctic cyclone in June 2008 simulated by the cloud resolving model NICAM. *Meteorol. Atmos. Phys..*, **137(660)**, 105-117.

Aizawa, T., and H. L. Tanaka, 2016: Axisymmertic structure of the long lasting summer cyclones. *Polar Science*, **10**, 192-198.

Bjerknes, J., and H. Solberg, 1922: Life cycle of cyclones and the polar front theory of atmospheric circulation. *Geophys. Publ.*, **3**, 1-18.

Browning, K. A., and N. M. Roberts, 1994: Structure of frontal cyclone. *Q. J. R. Meteorol. Soc.*, **120**, 1535-1557.

Browning, K. A., 1997: The dry intrusion perspective of extra-tropical cyclone development. *Meteorol. Appl.*, **4**, 317-324.

Catto, J. L., 2016: Extatropical cyclone classification and its use in climate studies. *Rev. Geophys.*, **54**, 486-520.

Cavalieri, D. J., C. L. Parkinson, and K. Y. Vinnikov, 2003: 30-year satellite record reveals contrasting Arctic and Antarctic decadal sea ice variability. *Geophys. Les. Lett.*, **30:1970**, doi:10.1029/2003GL018031.

Cavallo, S. M., and G. J. Hakim, 2009: Potential vorticity diagnosis of a tropopause polar cyclone. *Mon. Wea. Rev.*, **137**, 1358-1371.

Cavallo, S. M., and G. J. Hakim, 2010: Composite structure of tropopause polar cyclones. *Mon. Wea. Rev.*, **138**, 3840-3857.

Curry, J. A., W. B. Rossow, D. Randall, and J. L. Schram, 1996: Overview of Arctic cloud and radiation characteristics. *J. Climate*, **9**, 1731-1764.

Deveson, A. C. L., K. A. Browning, and T. D. Hewson, 2002: A classification of FASTEX cyclones using a height-attributable quasi-geostrophic vertical motion diagnostic. *Q. J. R. Meteorol. Soc.*, **128**, 93-117.

Ertel, H., 1942: Ein neuer hydrodynamischer Wirbelsatz. *Meteorology Zeitschr Braunchweis* , **59**, 271-281.

Field, P. R., and R. Wood, 2007: Precipitation and cloud structure in midlatitude cyclone. *J. Climate*, **20**, 233-254.

Grabowski, W. W., 1998: Toward cloud resolving modeling of largescale tropical circulations: a simple cloud microphysics parameterization. *J. Atmos. Sci.*, **55**, 3283-3298.

Hadlock, R., and C. W. kreitzberg, 1988: The Experiment on Rapidly Intensifying Over the Atlantic (ERICA) field study: Obsevationas and plans. *Bull. Am. Meteorol. Soc.*, **69**, 1309-1320.

Hakim, G. J., L.F. Bosart, and D. Keyser, 1995: The Ohio valley wave-merger cyclogenesis event of 25-26 January 1978. Part I: Multiscale case study. *Mon. Wea. Rev.*, **123**, 2663-2692.

Hewson, T.D., and U. Neu, 2015: Cyclones, windstorm and the IMILAST project. *Tellus A, 67A.*, 27128, doi:10.3402/tellusa.v67.27128.

Hoskins, B. J., M. E. McIntyre, and A. W. Robertson, 1985: On the use and significance of isentropic potential vorticity maps. *Q. J. R. Meteorol. Soc.*, **111**, 877-846.

Hoskins, B. J., 2015: Potntial vorticity and the PV perspective. *Adv. Atmos. Sci.*, **32**, 2-9.

Inoue, J., and M. E. Hori, 2011: Arctic cyclogenesis at the marginal ice zone: A contributory mechanism for the temperature amplification? *Geophys. Res. Lett*, **38**, L12502, doi:10.1029/2011GL047696.

Joly, A., and Co-authors, 1997: The Fronts and Atlantic Storm-Track Experiment (FASTEX): Scientific objectives and experimental design. *Bull. Am. Meteorol. Soc.*, **78**, 1917-1940.

Joly, A., and Co-authors, 1999: Overview of the field phase of the Fronts and Atlantic Storm-Track EXperiment (FASTEX) project. *Q. J. R. Meteorol. Soc.*, **125**, 3131-3165.

LeDrew, E.F., 1984: The role of local heat sources in synoptic activity in the Arctic Basin. *Atmos. Ocean*, **22**, 309-327.

LeDrew, E.F., 1987: Development processes for five depression systems within the Polar Basins. *J. Clim, Appl. Meteorol.*, **8**, 125-153.

LeDrew, E.F., 1989: Mode of synoptic development within the Polar Basin. *Geojournal*, **18**, 79-85.

Morgan, M.C., and J.W. Nielsen-Gammon, 1998: Using tropopause maps to diagnose midlatitude weather systems. *Mon. Wea. Rev.*, **126**, 2555-2579.

Nakanishi, N., and H. Niino, 2004: An improved Mellor-Yamada Level-3 model with condensation physics: its design and velification. *Bound. Layer Meteorol.*, **112**, 1-31.

Petterseen, S., and S. J. Smebye, 1971: On the development of extratropical cyclones. *Q. J. R. Meteorol. Soc.*, **97**, 457-482.

Posselt, D.J., and J.E. Martin, 2004: The effect of latent heat release on the evolution of a warm occluded thermal structure. *Mon. Wea. Rev.*, **132**, 578-599.

Randel, W. J., F. Wu, and P. Forester, 2007: The extratropical tropopause inversion layer: Grobal observations with GPS data, and a radiative forcing mechanism. *J. Atmos. Sci.*, **64**, 4489-4496.

Rigor, I.G., R.L. Colony, and S. Martin, 2000: Variations in surface air temperature observations in the Arctic, 1979-97. *J. Climate*, **13**, 896-914.

Sanders, F., and F. R. Gyakum, 1980: Synoptic-dynamic climatology of the "Bomb". *Mon. Wea. Rev.*, **108**, 1589-1606.

Satoh, M., T. Matsuno, H. Tomita, H. Miura, T. Nasuno, and S. Iga, 2004: Nonhydrostatic ICosahedral Atmospheric Model (NICAM) for global cloud-resolving simulation. *J. Comput. Phys.*, **227**, 3486-3514.

Schults, D. M., D. Keyser, and L. F. Bosart, 1998: The effect of large-scale flow on low-level frontal structure and evolution in mid-latitude cyclones. *Mon. Wea. Rev.*, **126**, 1767-1791.

Schults, D. M., and G. Vaughan, 2011: Occluded fronts and the occlusion process: A fresh look at conventional wisdom. *Bull. Amer. Meteor. Soc.*, **92**, 443-466.

Serreze, M. K., A. M. Lynch, and M. P. Clark, 2001: The arctic frontal zone as seen in NCEP-NCAR reanalysis. *J. Climate*, **14**, 1550-1567.

Serreze, M. K., and A. P. Barrett, 2007: The summer cyclone maximum over the central Arctic Ocean. *J. Climate*, **21**, 1048-1065.

Shapiro, M. A., and D. keyser, 1986: A review of the structure and dynamics of upper-level frontal zone. *Mon. Wea. Rev.*, **118**, 452-499.

Shapiro, M. A., and D. keyser, 1990: Fronts, jet streams and the tropopause. Extratropical cyclones *The Erik Palmen Memorial Volume, C. Newton and E. O. Holopainen, Eds, Amer. Meteor. Soc.*, 167-191.

Simmonds, I., C. Burke, and K. Keay, 2008: Arctic climate change as manifest in cyclone behavior. *J. Climate*, **21**, 5777-5796.

Simmonds, I., and K. Rudeva, 2012: The great Arctic cyclone of August 2012. *Geophys. Res. Lett.*, **39**, L23709, doi:10.1029/2012GL054259.

Stoelinga, M. T., 1996: A potential vorticity-based study of the role of diabatic heating and friction in a numerically simulated baroclinic cyclone. *Mon. Wea. Rev.*, **124**, 849-874.

Stroeve, J. C., M. M. Holland, W. Meier, T. Scambos, and M. Serreze, 2007: Arctic sea ice decline: faster than forecast. *Geophys. Les. Lett.*, **32:L09501**, doi:10.1029/2007GL029703.

Tanaka, H. L., A. Yamagami, and S. Takahashi, 2012: The structure and behavior of the Arctic cyclone analyzed by the JRA-25/JCDAS data. *Polar Science*, **6**, 54-69.

Thorncroft, C. D., B. J. Hoskins, and M. E. McIntyre, 1993: Two paradigms of baroclinic-wave life-cycle behaviour. *Q. J. R. Meteorol. Soc.*, **119**, 17-55.

Thorpe, A.J., 1986: Synoptic scale disturbances with circular symmetry. *Mon. Wea. Rev.*, **114**, 1384-1389.

Wang, C. C., and J. C. Rogers, 2001: A composite study of explosive cyclogenesis in different sectors of the North Atlantic. Part I: Cyclone structure and evolution. *Mon. Wea. Rev.*, **129**, 1481-1499.

Wernli, H., S. Dirren, M. A. Linger, M. Zillig, 2002: Dynamics aspects of the life cycle of the winter storm 'Lothar' (24-26 December 1999). *Q. J. R. Meteorol. Soc.*, **128**, 405-429.

Wirth, V., 1995: Diabatic heating in an axisymmetric cut-off cyclone and related stratosphere-troposphere change. *Q. J. R. Meteorol. Soc.*, **121**, 127-147.

Zhang, X., J.E. Walsh, J. Zhang, U. S. Bhatt, and M. Ikeda, 2004: Climatology and interannual variability of Arctic cyclone activity: 1948-2002. *J. Climate*, **17**, 2300-2317.

Table 1: Layer averaged potential temparature budget between 100 and 300 hPa from 00Z, 10 June to 00Z, 11 June in the appearing phase for the case 2008.

	Change rate	Contributing rate
Layer averaged potential temperature	3.3 K	
Horizontal advection	2.7 K	80 %
Adiabatic effect	3.0 K	92 %
Diabatic effect	-2.4 K	-72 %

Table 2: Layer averaged potential temparature budget between 100 and 300 hPa from 18Z, 19 June to 06Z, 22 June in the rapid intensification phase for the case 2008.

	Change rate	Contributing rate
Layer averaged potential temperature	3.0 K	
Horizontal advection	2.1 K	70 %
Adiabatic effect	3.6 K	119 %
Diabatic effect	-2.7 K	-89 %

Table 3: Layer averaged potential temparature budget between 300 and 925 hPa from 00Z, 10 June to 00Z, 11 June in the appearing phase for the case 2008.

	Change rate
Layer averaged potential temperature	0.2 K
Horizontal advection	-0.4 K
Adiabatic effect	-2.1 K
Diabatic effect	2.7 K

Table 4: Layer averaged potential temparature budget between 300 and 925 hPa from 00Z, 11 June to 06Z, 18 June in the weakening phase for the case 2008.

	Change rate
Layer averaged potential temperature	-3.5 K
Horizontal advection	2.9 K
Adiabatic effect	0.2 K
Diabatic effect	-6.6 K

Table 5: Layer averaged potential temparature budget between 300 and 925 hPa from 18Z, 19 June to 06Z, 22 June in the rapid intensification phase for the case 2008.

	Change rate	Contributing rate
Layer averaged potential temperature	3.0 K	
Horizontal advection	6.9 K	226 %
Adiabatic effect	-3.8 K	-124 %
Diabatic effect	-0.1 K	-2 %

Table 6: Layer averaged potential temparature budget between 100 and 300 hPa from 00Z, 5 August to 18Z, 7 August in the merging and maintenance phases for the case 2012.

	Change rate	Contributing rate
Layer averaged potential temperature	17.4 K	
Horizontal advection	12.1 K	70 %
Adiabatic effect	10.3 K	59 %
Diabatic effect	-5.1 K	-29 %

Table 7: Layer averaged potential temparature budget between 300 and 925 hPa from 00Z, 5 August to 18Z, 7 August in the merging and maintenance phases for the case 2012.

	Change rate	Contributing rate
Layer averaged potential temperature	-13.3 K	
Horizontal advection	-3.6 K	27 %
Adiabatic effect	-12.2 K	92 %
Diabatic effect	2.5 K	-19 %

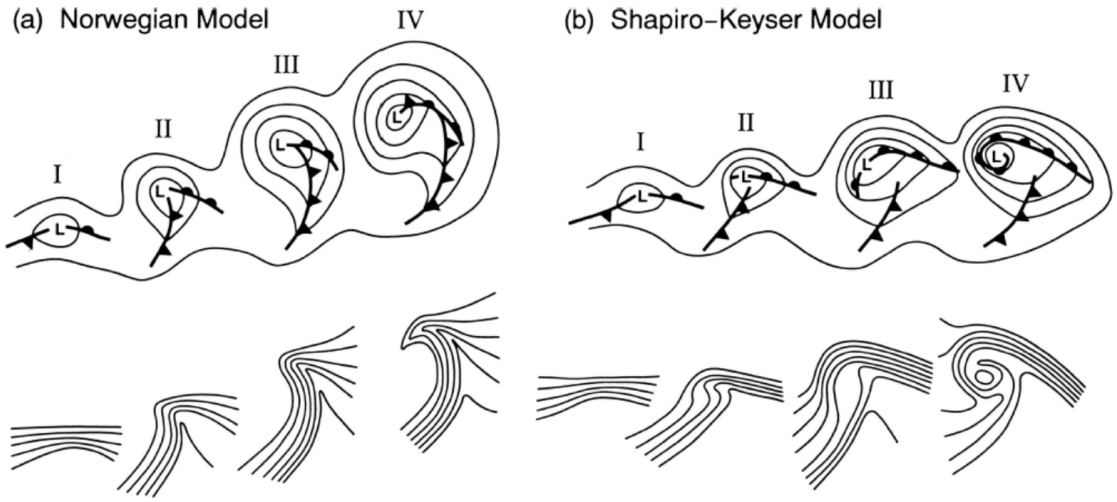

Fig. 1: Conceptual models of cyclone evolution showing lower-tropospheric (e.g., 850-hPa) geopotential height and fronts (top), and lower-tropospheric potential temperature (bottom). (a) Norwegian cyclone model: (I) incipient frontal cyclone, (II) and (III) narrowing warm sector, (IV) occlusion; (b) Shapiro.Keyser cyclone model: (I) incipient frontal cyclone, (II) frontal fracture, (III) frontal T-bone and bent-back front, (IV) frontal T-bone and warm seclusion. Panel (b) is adapted from Shapiro and Keyser (1990, their Fig. 10.27) to enhance the zonal elongation of the cyclone and fronts and to reflect the continued existence of the frontal T-bone in stage IV. The stages in the respective cyclone evolutions are separated by approximately 6-24 h and the frontal symbols are conventional. The characteristic scale of the cyclones based on the distance from the geopotential height minimum, denoted by L, to the outermost geopotential height contour in stage IV is 1000 km. (from Schults et al. 1998)

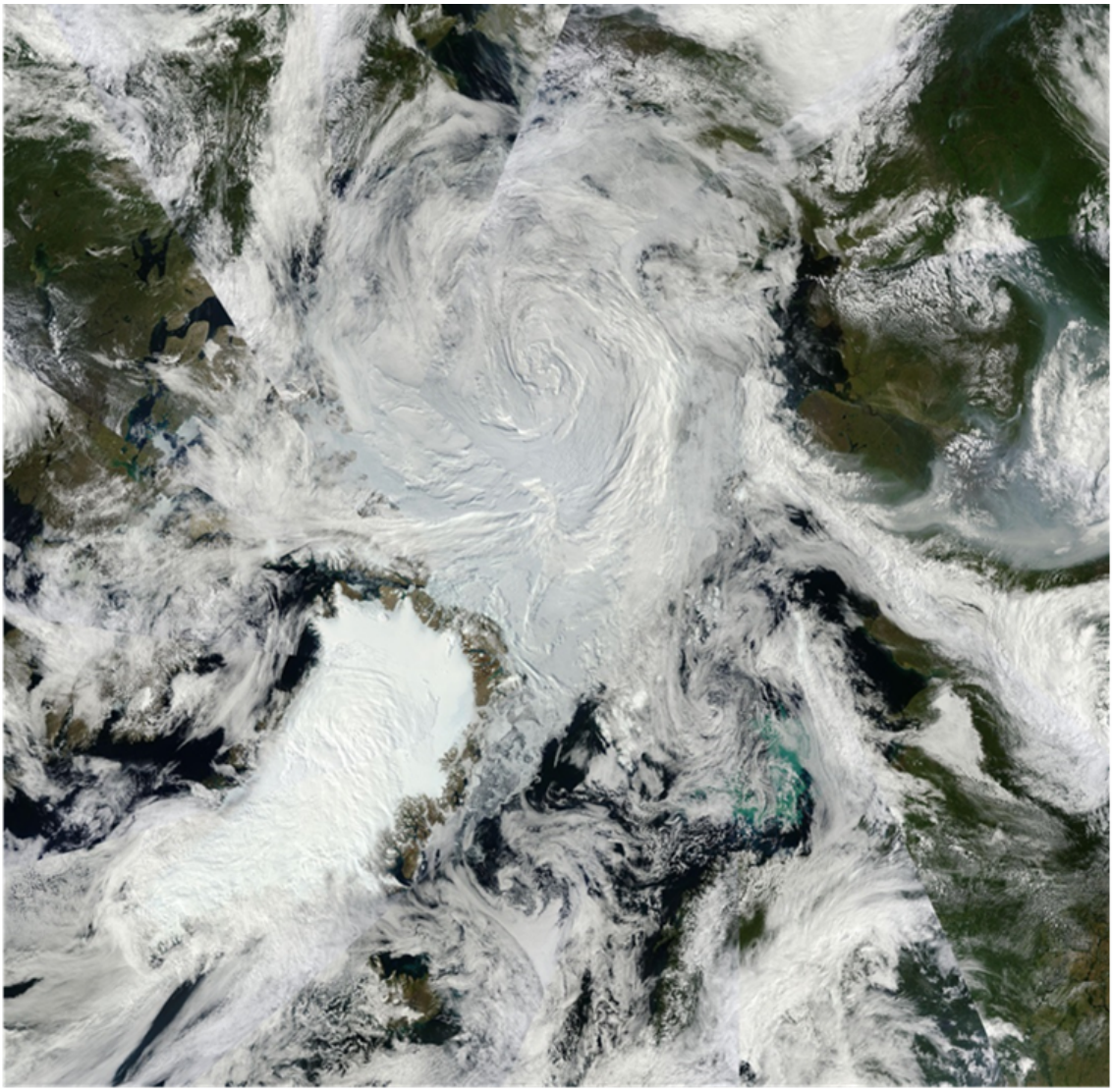

Fig. 2: Satellite image in the Arctic on 5 August 2012.

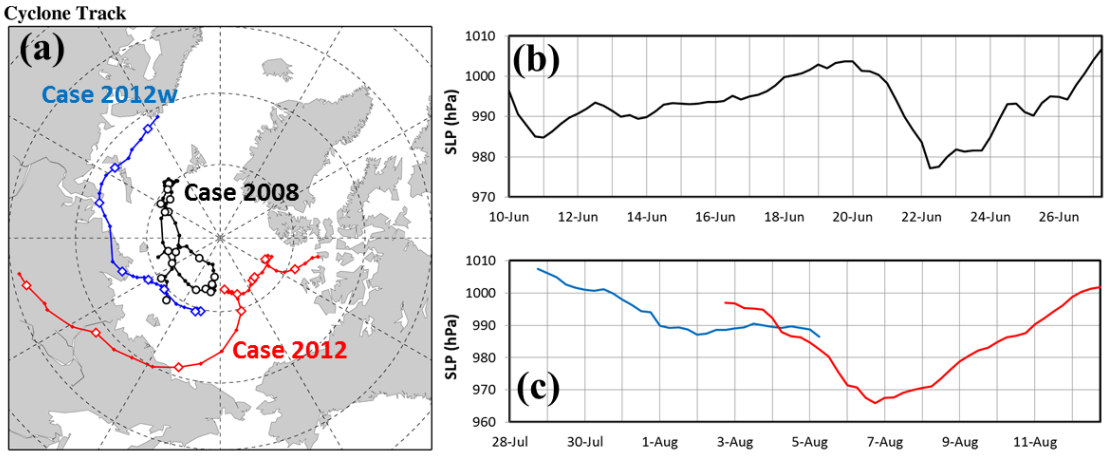

Fig. 3: Tracks of the Arctic cyclones, and time series of the minimum central pressures for (b) the case 2008, (c) the case 2012 (red line) and the 2012w (blue line).

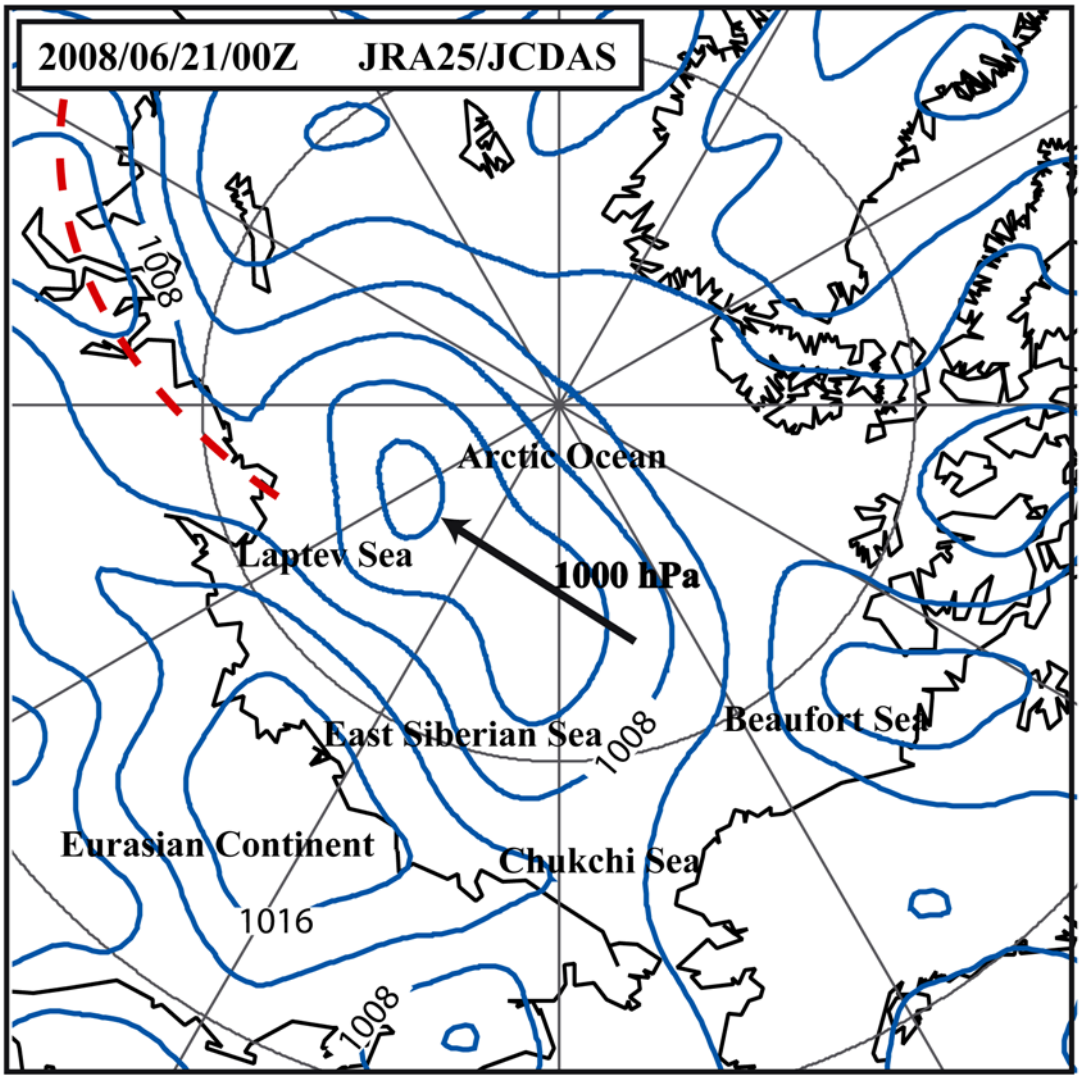

Fig. 4: Horizontal plot of the sea level pressures of JRA25/JCDAS on 00Z, 21 June 2008. The contour interval is 4 hPa. The geographical names are described. An arrow indicates a target cyclone of this study, and a dashed line shows a local front in the Arctic.

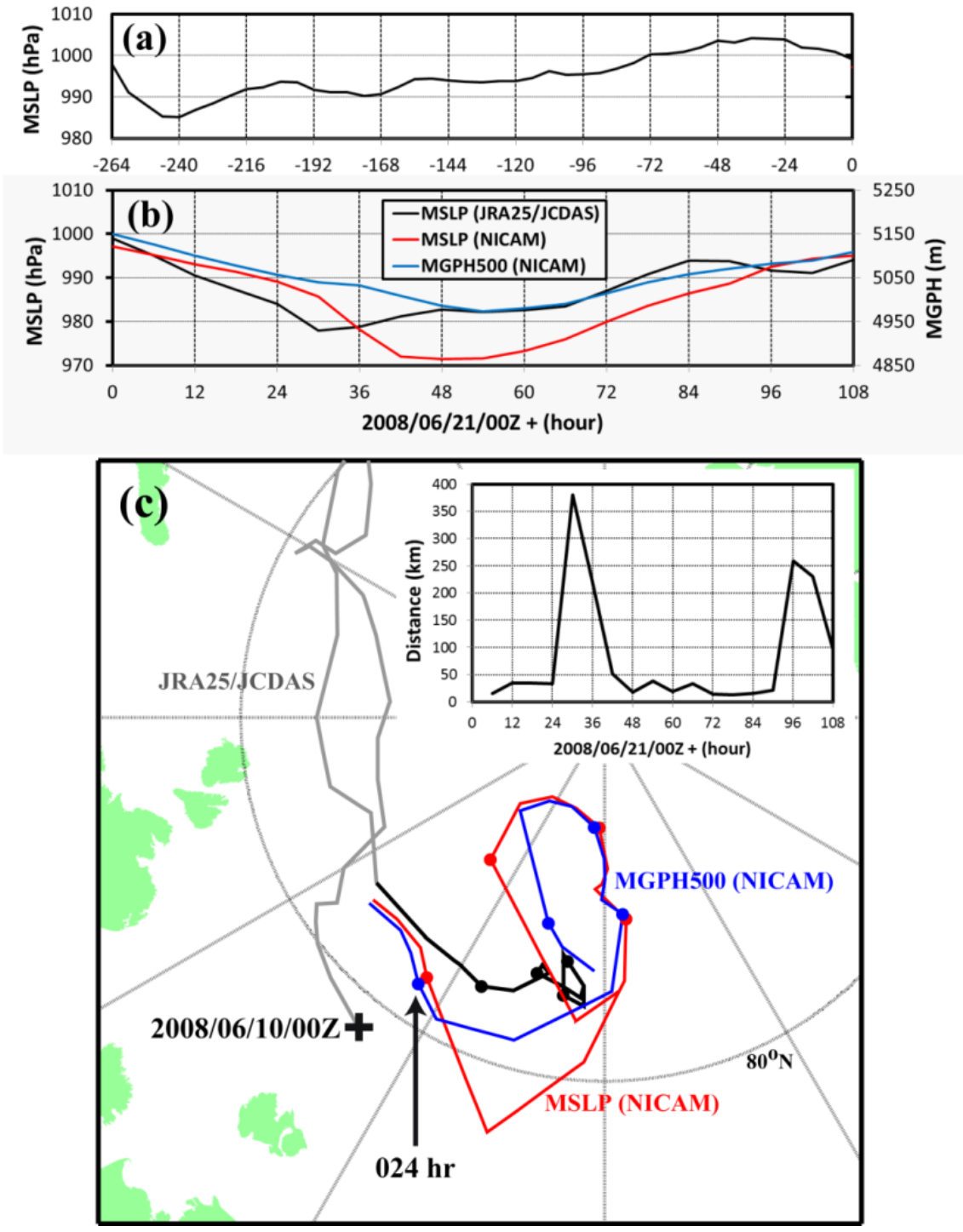

Fig. 5: Time series of (a) Minimum sea level pressure (MSLP) of a target cyclone by the JRA25/JCDAS from 00Z, 10 June 2008 to 00Z, 21 June, (b) MSLP and minimum geopotential height at 500 hPa of a simulated cyclone, and MSLP by the JRA25/JCADS from 00Z, 21 June 2008. (c) illustrates the cyclone tracks of simulation (blue and red lines) and JRA25/JCDAS (gray and black lines). A symbol of plus denotes a location of the genesis. An arrow indicates the cyclone centers of simulated cyclone at 024 hr. A time series in (c) shows the distances between cyclone centers at 500 hPa (MGPH500) and that at sea level (MSLP).

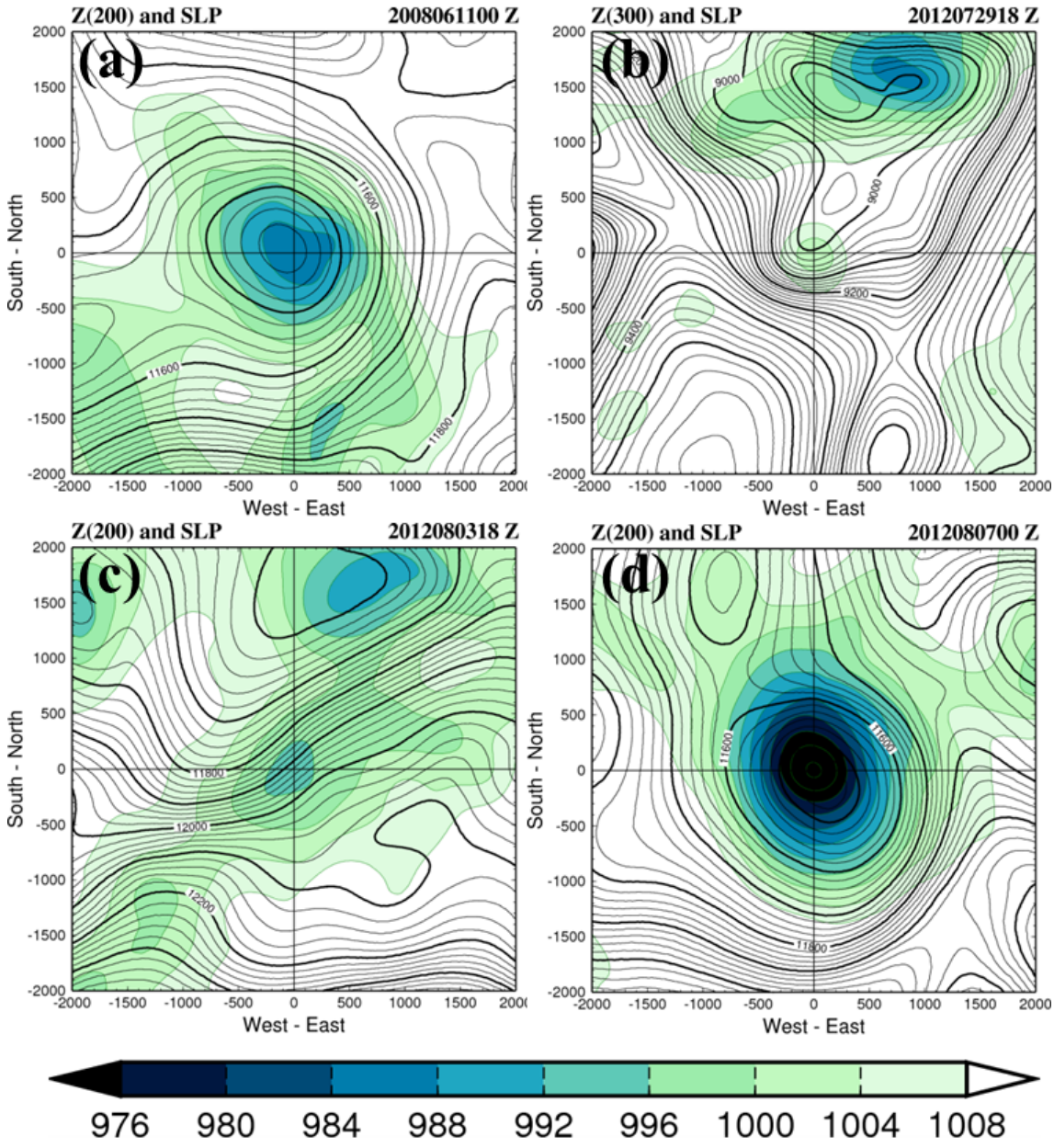

Fig. 6: The relationships between the lower stratospheric cyclones (200 or 300 hPa) and the surface cyclones after 24 hours from the cyclones appeared for (a) the case 2008, (b) the case 2012w and (c) the case 2012, and (d) the mature stage of the case 2012. The contours show the geopotential height at 200 hPa (a, c, d) and 300 hPa (b) with intervals of 40 m. The colors illustrate the sea level pressure.

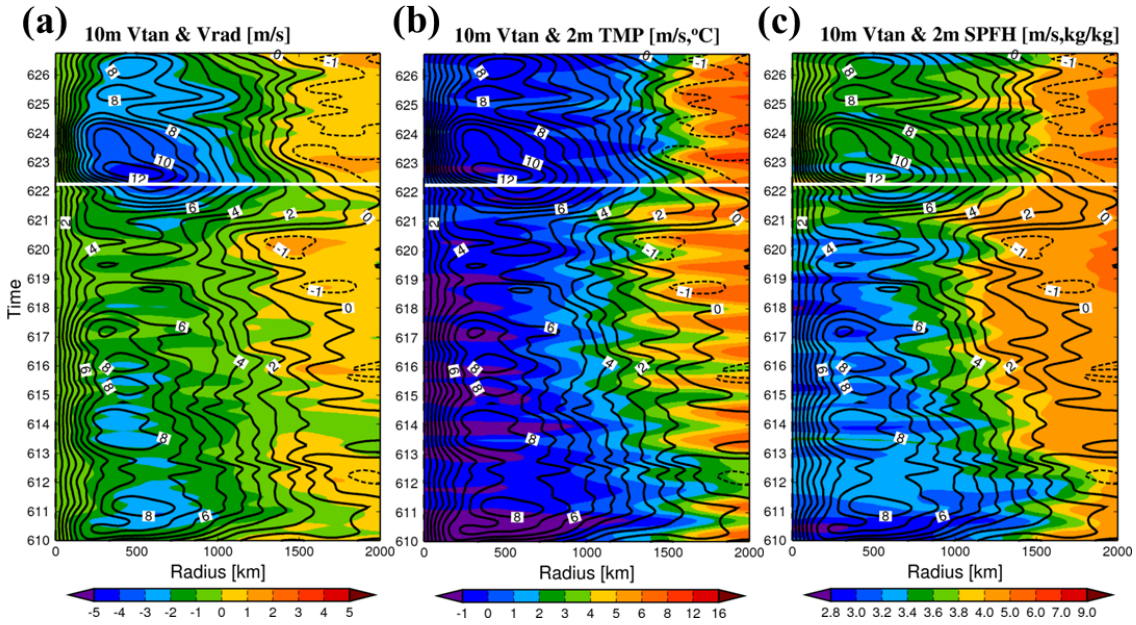

Fig. 7: Time-radius cross sections of azimuthal mean (a) tangential wind speed (m/s) and radial wind speed (m/s) at 10 m level, (b) air temperature (^{o}C) at 2 m level and (c) specific humidity (g/kg) at 2 m level for the case 2008. The tangential wind was indicated by the contour with 1 (m/s) interval. The radial wind, the temperature and the specific humidity are indicated by the color shades. The black lines in (b) and (c) indicate the tangential wind. The white lines mark a time when the minimum central pressure of the cyclone was the lowest. (For interpretation of the references to colour in this figure legend, the reader is referred to the web version of this article.)

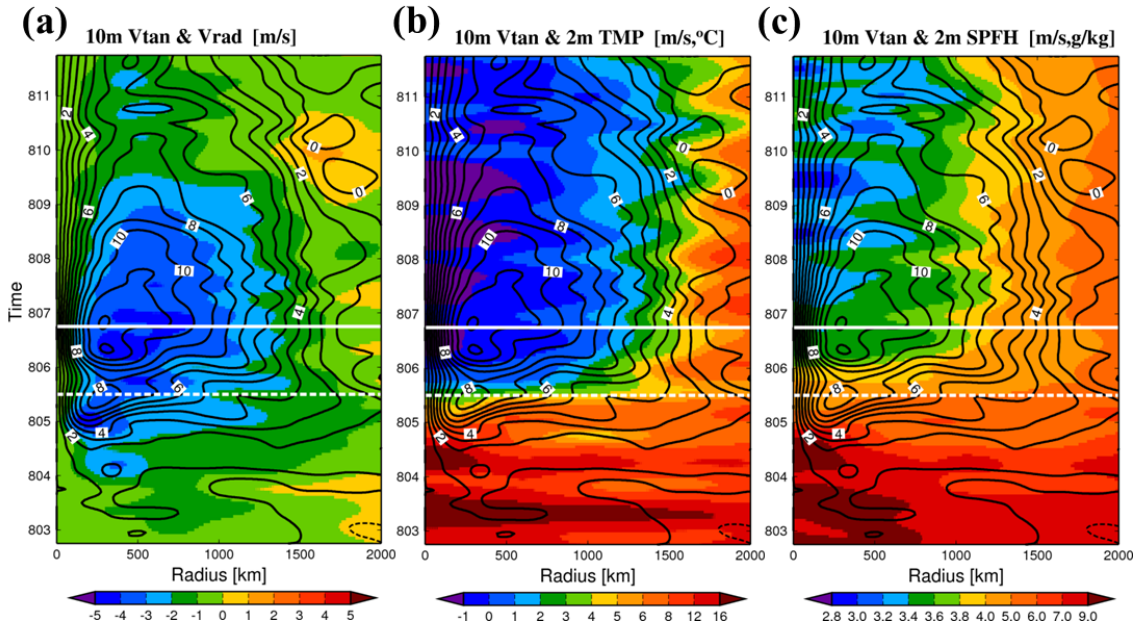

Fig. 8: Same as Fig. 7, but for the case 2012. The dashed white lines mark a time when the two surface cyclone systems merged.

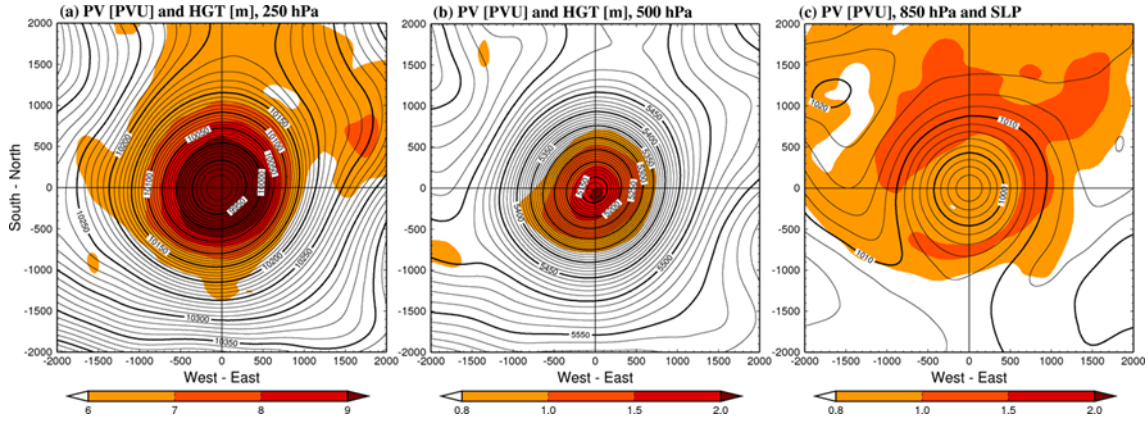

Fig. 9: Time averaged potential vorticity (PVU) at (a) 250 hPa, (b) 500hPa and (c) 850 hPa, geopotential height (m) at (a) 250 hPa, (b) 500hPa and (c) sea level pressure (hPa) for the case 2008. The figures are time average during the life cycle (00Z 10 June - 18Z 26 June, 2008). The shades show the potential vorticity, and the contours show the geopotential height (a, b) and sea level pressure (c). The contour interval in (a), (b) and (c) is 20 (m/s) and 2 hPa, respectively. The thick lines highlight the geopotential heights every 200 m and sea level pressures every 10 hPa.

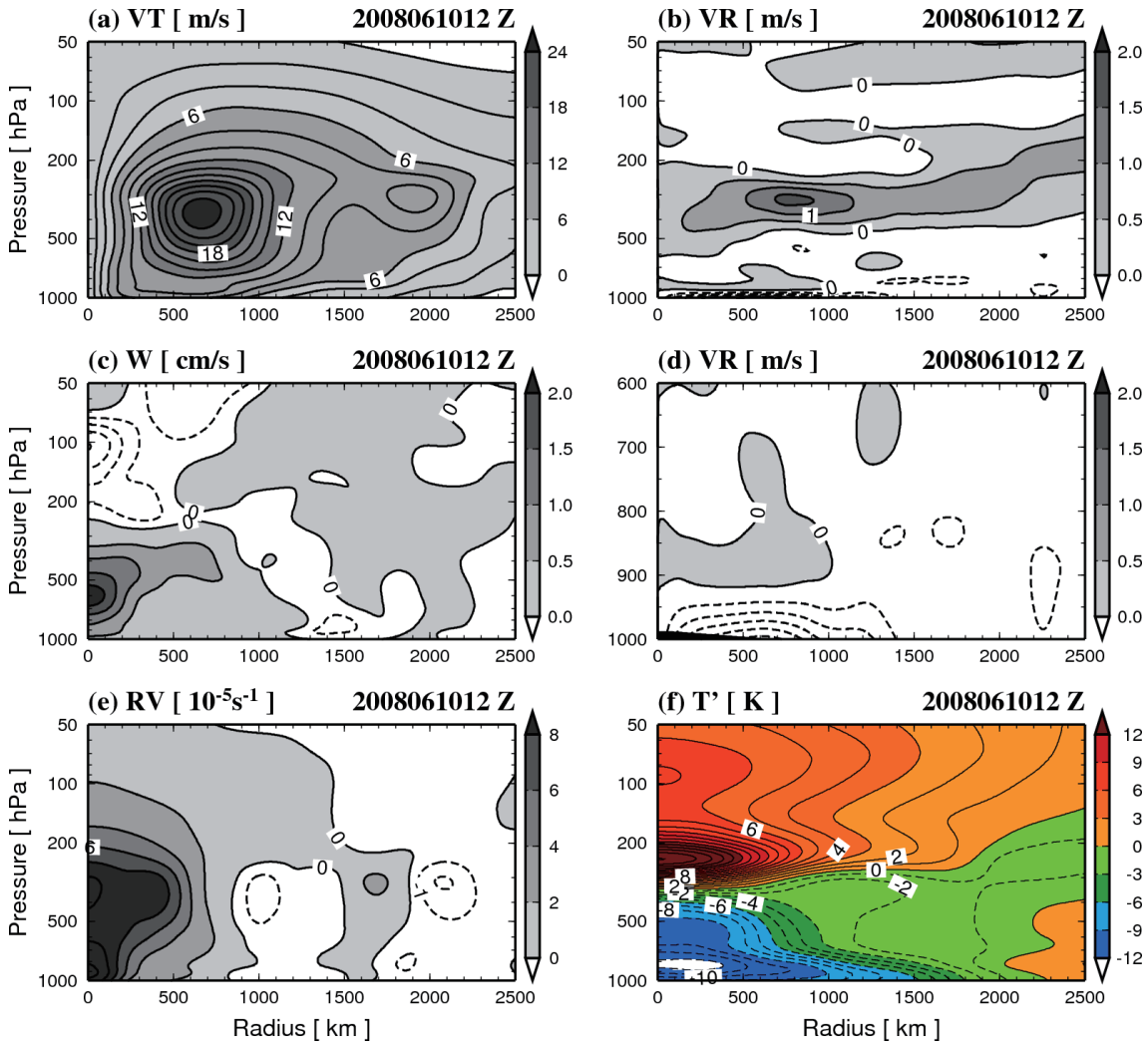

Fig. 10: Radius-height cross sections of azimuthal mean (a) tangential wind speed (m/s), (b) radial wind speed (m/s), (c) vertical velocity (cm/s), (d) enlarged plot of (b) near the surface (m/s), (e) relative vorticity (10^{-5} s^{-1}) and (f) temperature deviation (^{o}C) on 12Z 10 June for the case 2008. The situation of the cyclone is after 12 hours from the appearing. The bold contours indicate the dynamical tropopause (2.0 PVU surface). The solid lines and the dashed lines indicate positive and negative values. The intervals of the dashed line in (c), (b, d) and (e) are 0.03 (cm/s), 0.5 (m/s) and 1.0 (10^{-5} s^{-1}), respectively.

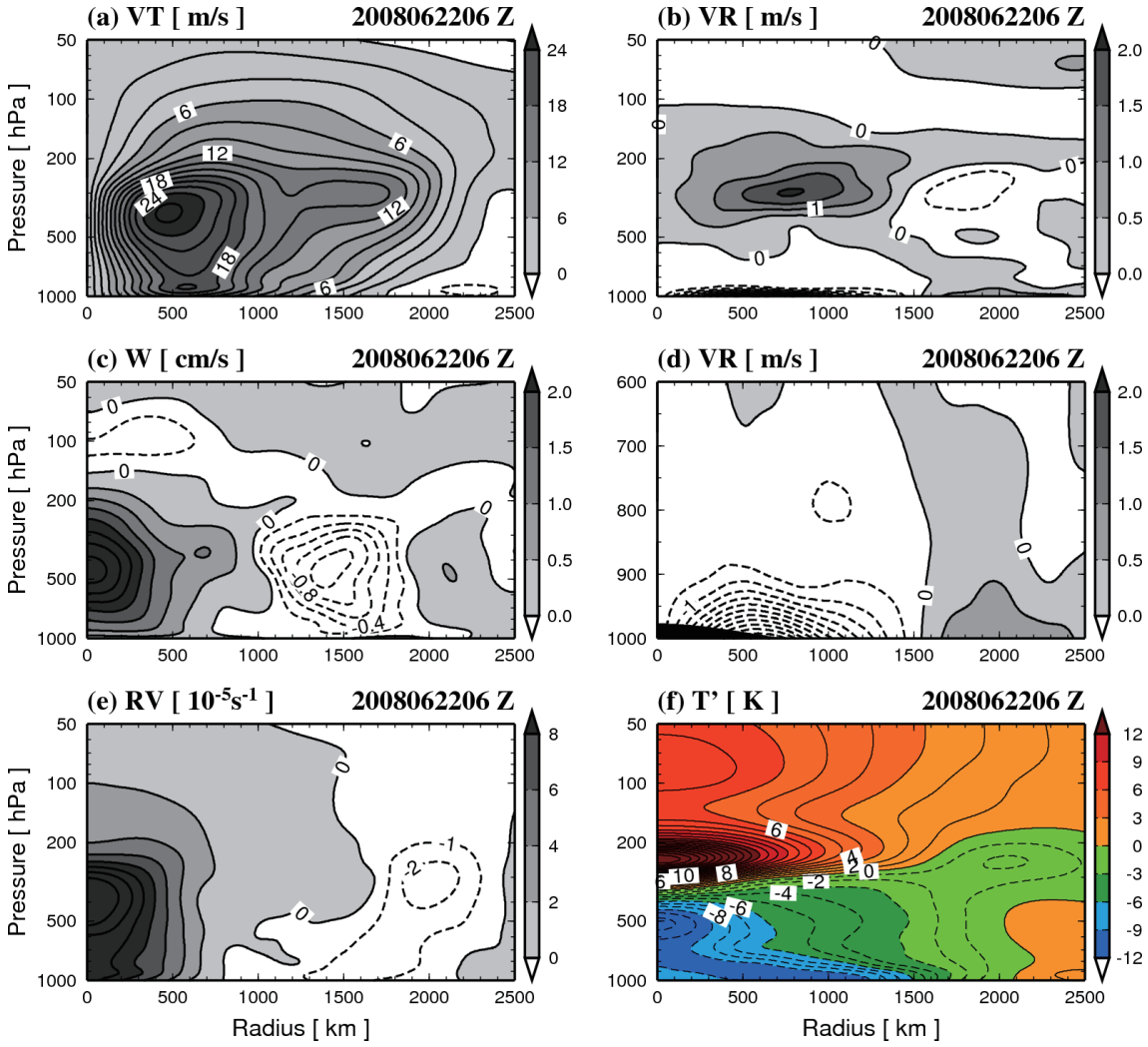

Fig. 11: Same as Fig. 10, but on 06Z 22 June. The situation of the cyclone is in the mature stage.

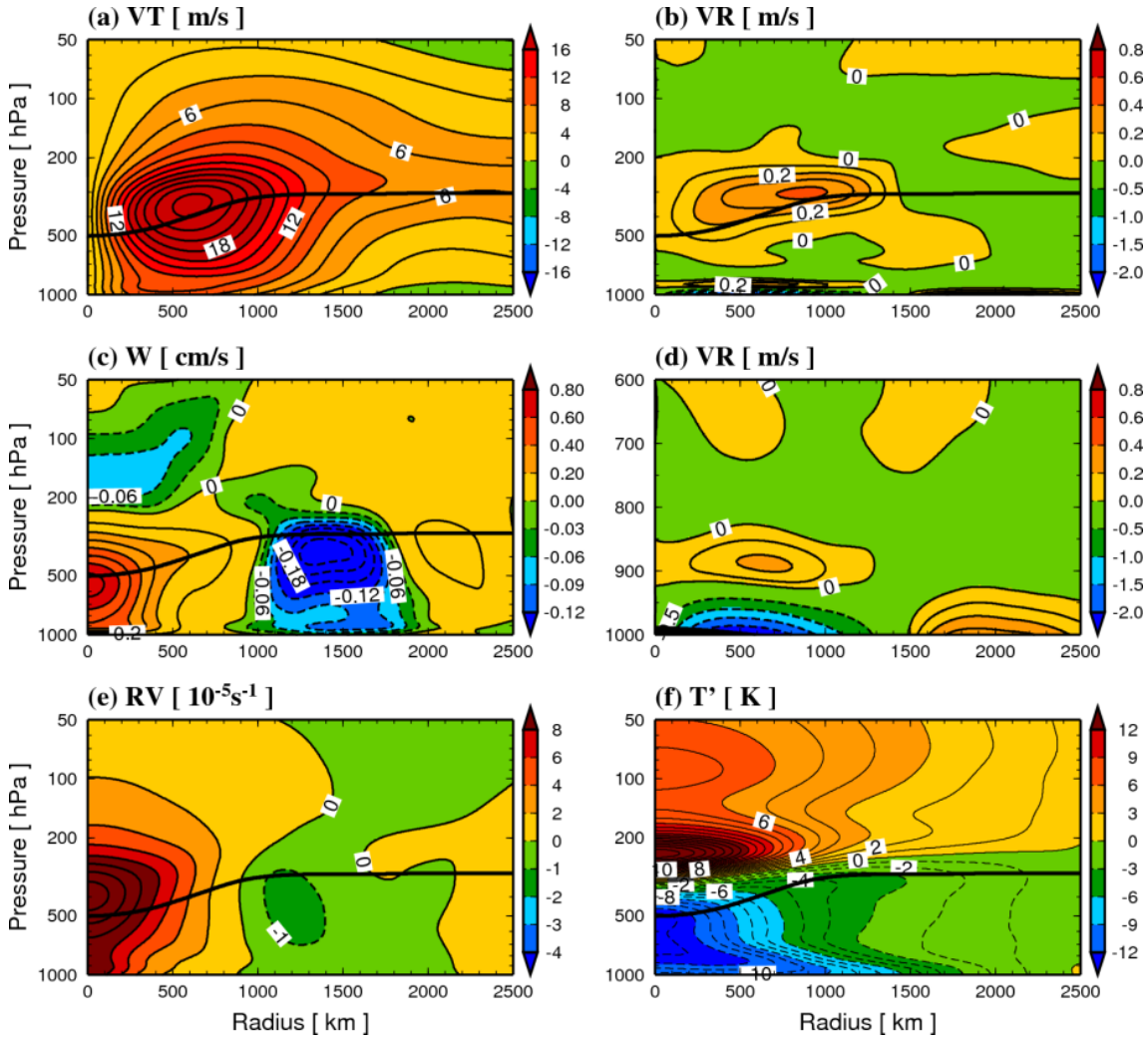

Fig. 12: Radius-height cross sections of azimuthal mean (a) tangential wind speed (m/s), (b) radial wind speed (m/s), (c) vertical velocity (cm/s), (d) enlarged plot of (b) near the surface (m/s), (e) relative vorticity (10^{-5} s^{-1}) and (f) temperature deviation (^{o}C) for the case 2008. The figures are time average during the life cycle (00Z 10 June e 18Z 26 June, 2008). The bold contours indicate the dynamical tropopause (2.0 PVU surface). The solid lines and the dashed lines indicate positive and negative values. The intervals of the dashed line in (c), (b, d) and (e) are 0.03 (cm/s), 0.5 (m/s) and 1 (10^{-5} s^{-1}), respectively.

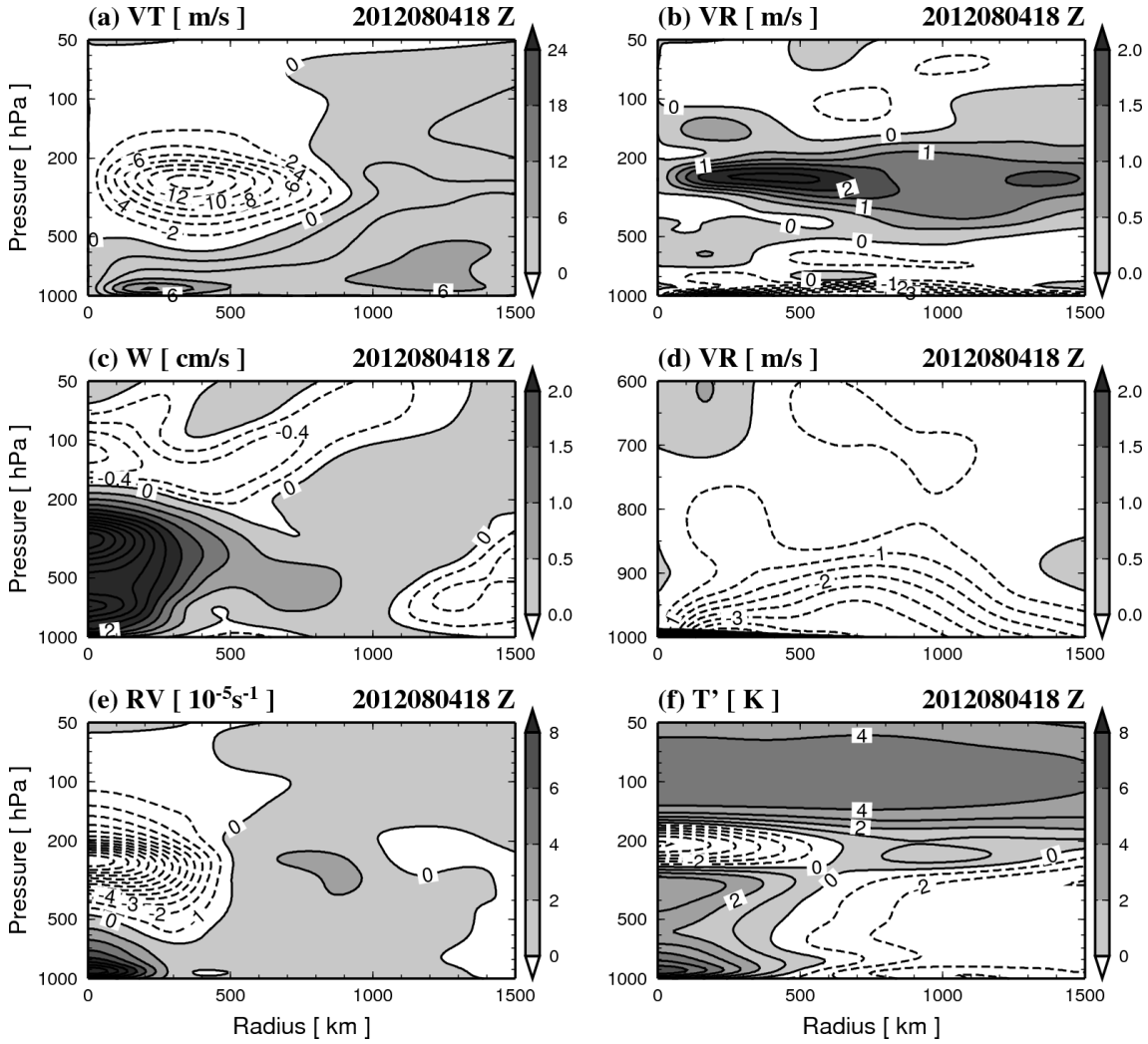

Fig. 13: Same as Fig. 10, but in the early developmental stage (18Z 4 August 2012) for the case 2012. The interval of the dashed line in (a) is 2 (m/s).

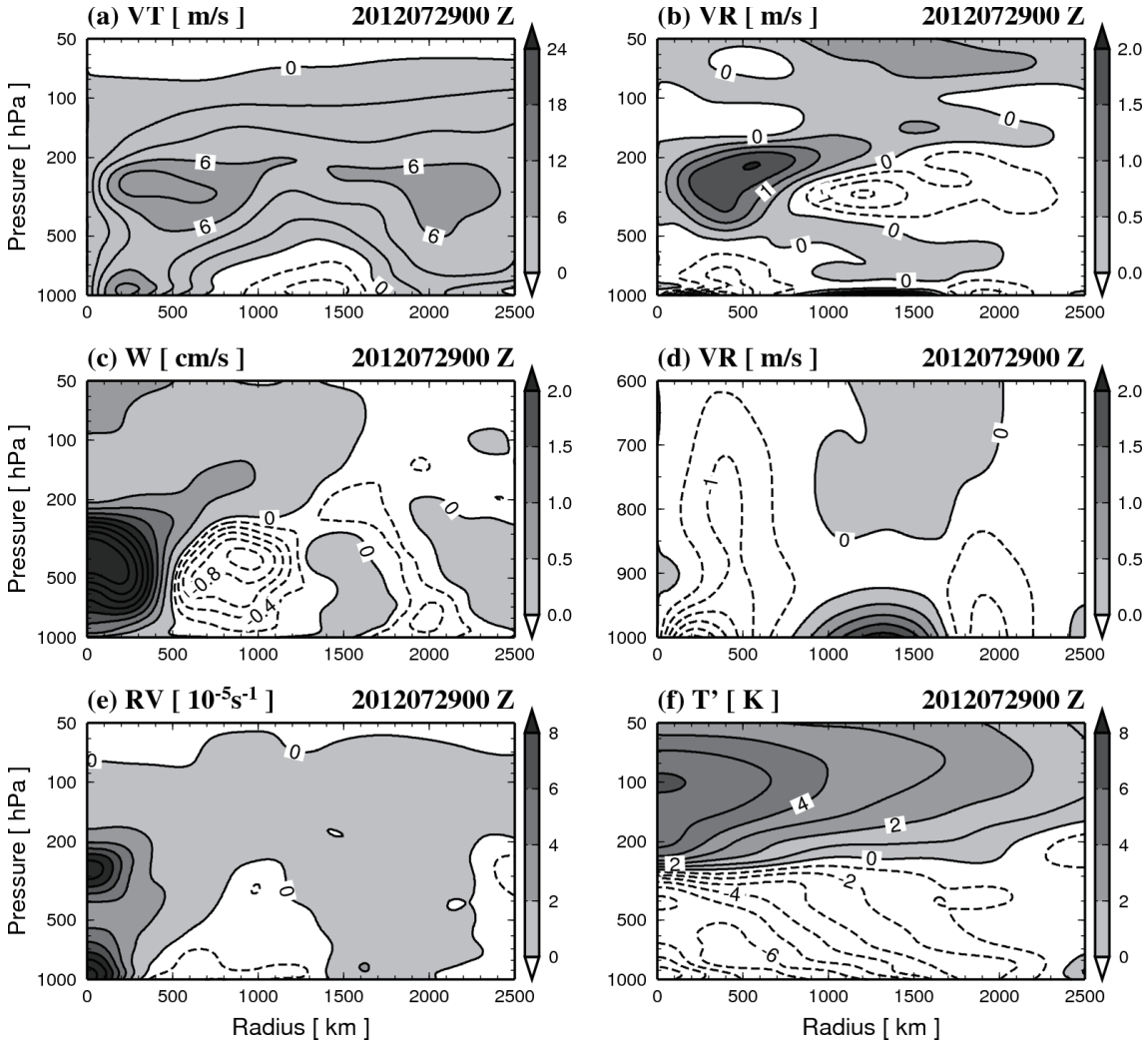

Fig. 14: Same as Fig. 10, but in the early developmental stage (06Z 29 July 2012) for the case 2012w. The interval of the dashed line in (a) is 2 (m/s).

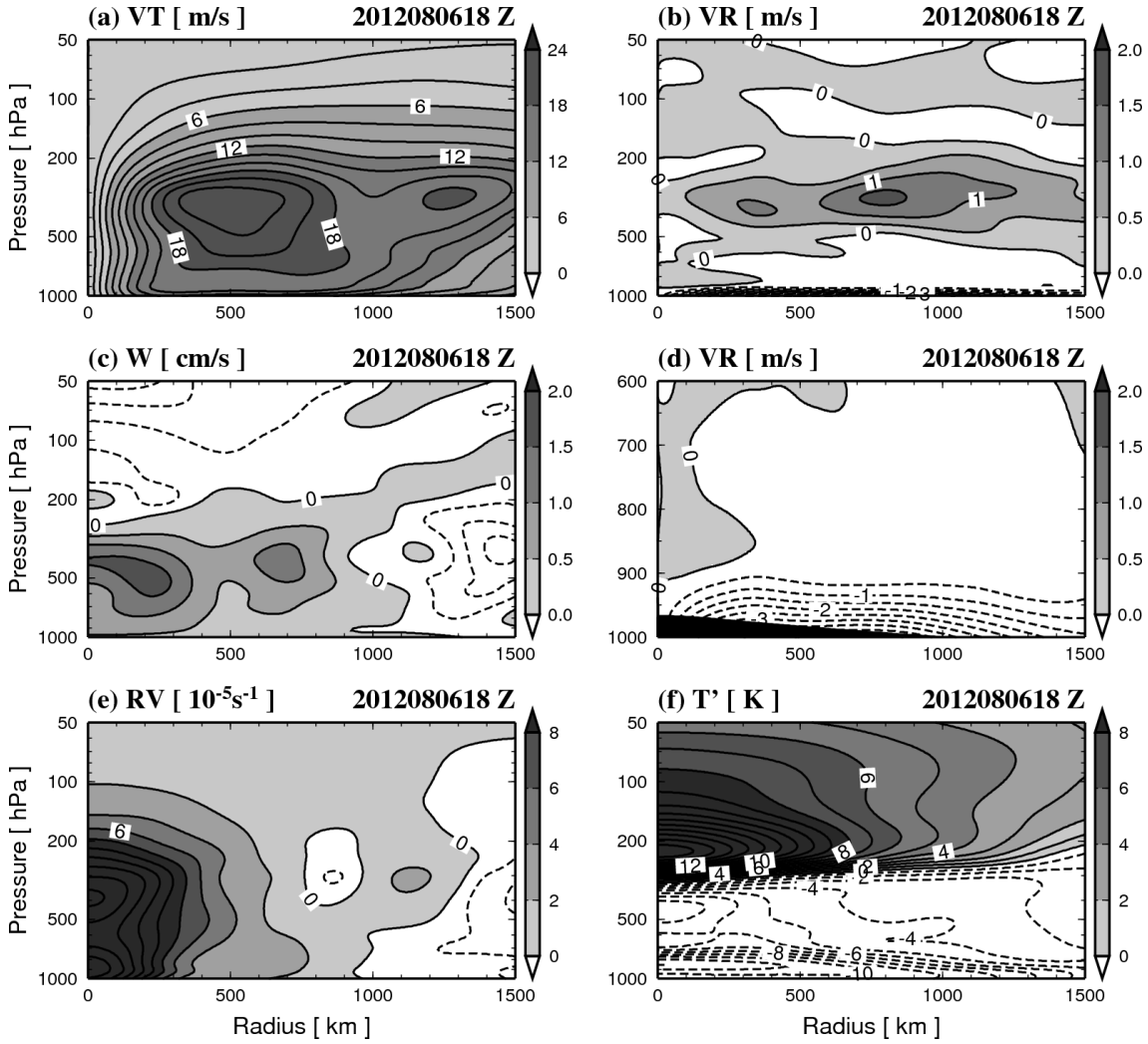

Fig. 15: Same as Fig. 10, but in the mature stage (18Z 6 August 2012) for the case 2012.

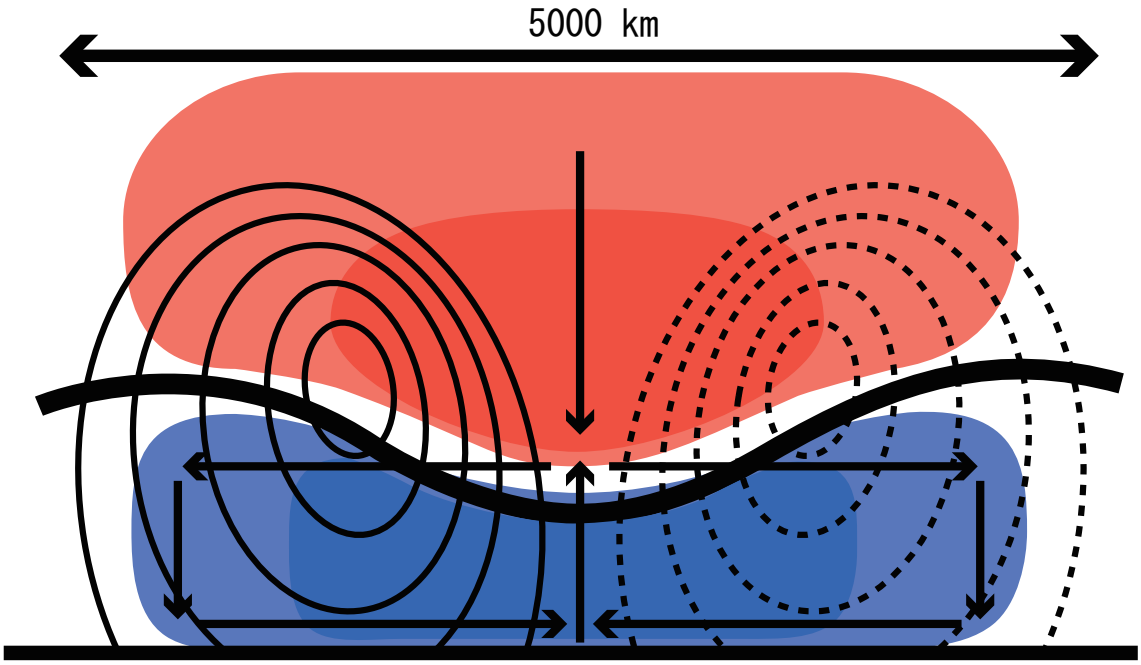

Fig. 16: Schematic diagram of the Arctic cyclones. The thin solid and dashed lines indicate the tangential wind jet and the opposite tangential wind jet, respectively, indicating the cyclonic circulation. A bold line indicates the tropopause. The warm core and cold core are shaded in red color and blue color, respectively. Black allows show the secondary circulation and the lower stratospheric downdraft.

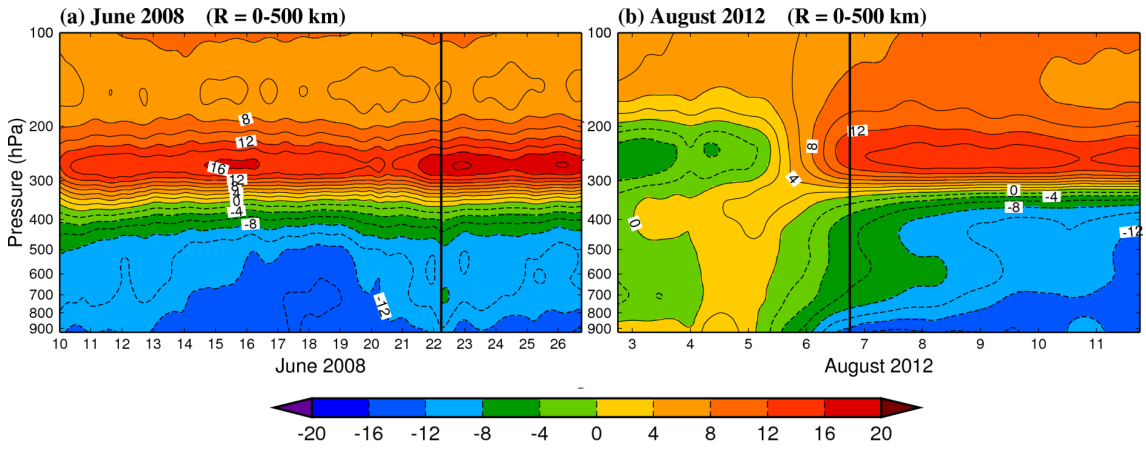

Fig. 17: Time-heigt cross section of the reginal mean temparature deviations (^{o}C) averaged in radius of 500 km calculated by sect. 2. (a) case of June 2008, (b) case of August 2012. The soild contours and the dashed contours indicate the positive values and the negative values with the interval of 2 (^{o}C). The warmer colors show the warm core anomalies.

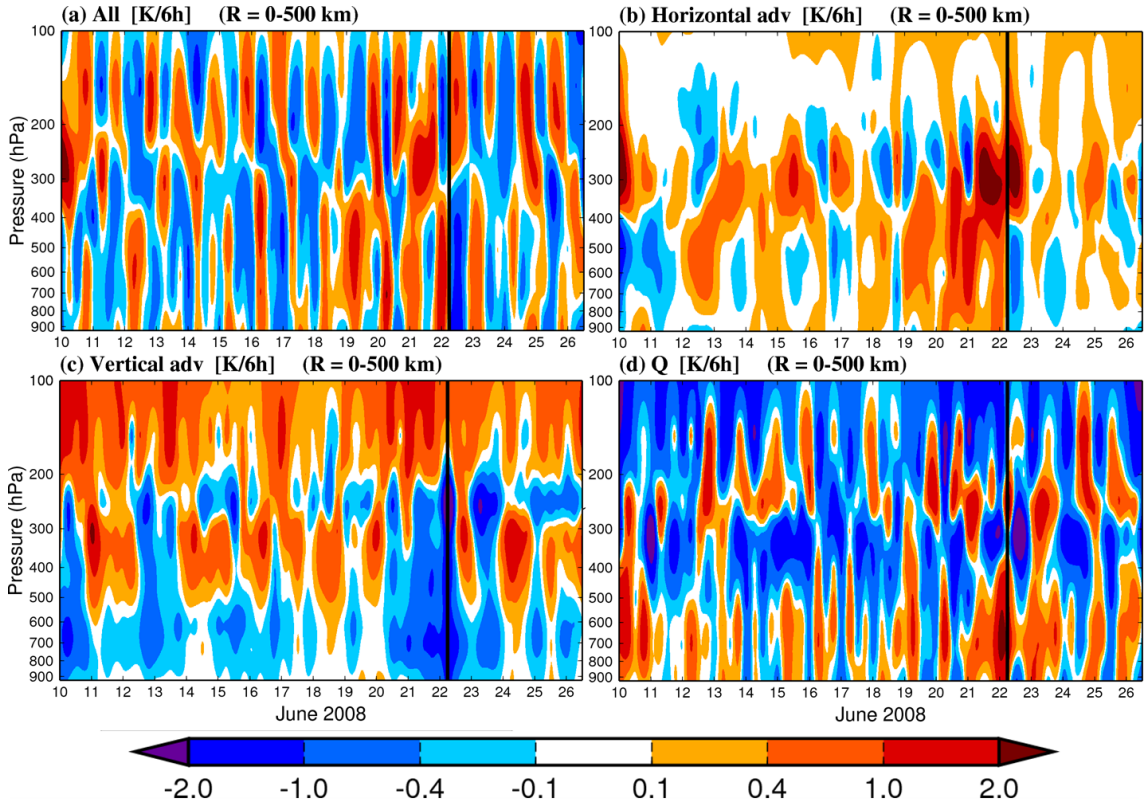

Fig. 18: Time-height cross section of (a) the potential temperature tendency term, (b) the horizontal advection term, (c) the adiabatic term by the vertical flows and (d) the diabatic term for the case 2008. Values are averaged in radius of 500 km from the cyclone centers. An unit of all figures is (K/6hour). A solid line on 6Z 22 June shows the cyclone was in the maximum intensity.

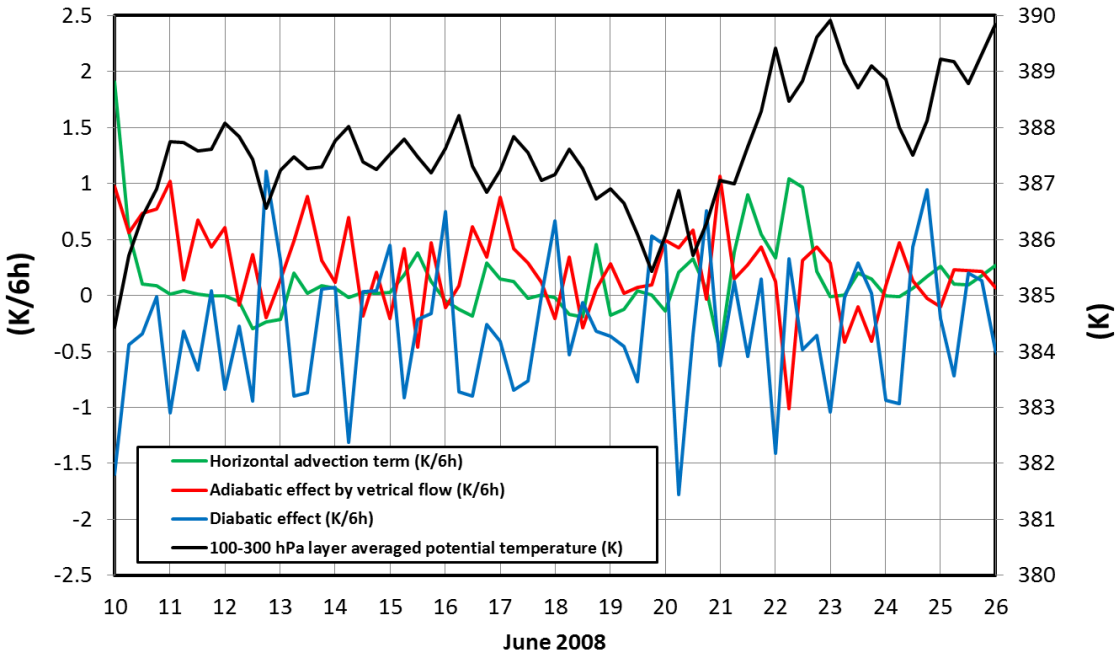

Fig. 19: Time series of the potential temperature budget averaged from 100 to 300 hPa level for the case 2008. A blcak line, blue line, red line and green line show the potential temperature (K), the horizontal advection term (K/6h), the adiabatic term by the vertical motion (K/6h) and the diabatic effecrts (K/6h), respectively.

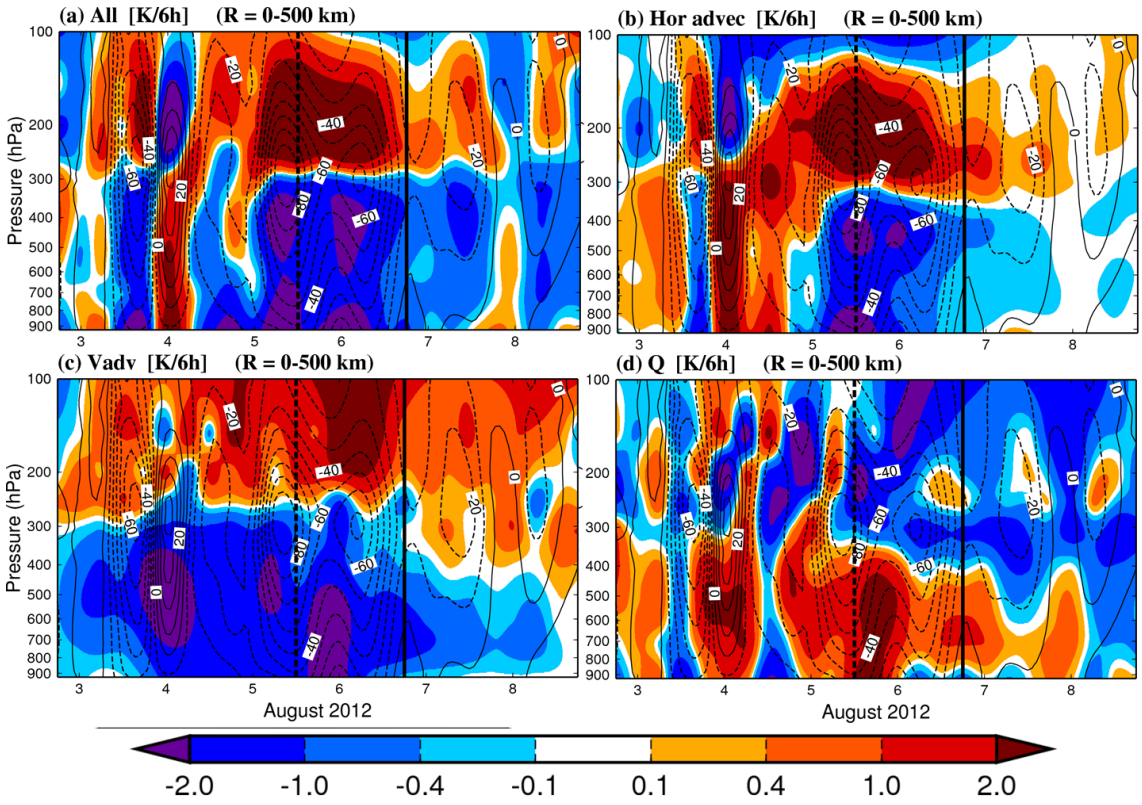

Fig. 20: Same as Fig.18, but for the case 2012. A solid line on 18Z 6 August shows the cyclone was in the maximum intensity. A dashed line on 12Z 5 August shows time when the cyclone merged with the pre-existing Arctic cyclone (case 2012w).

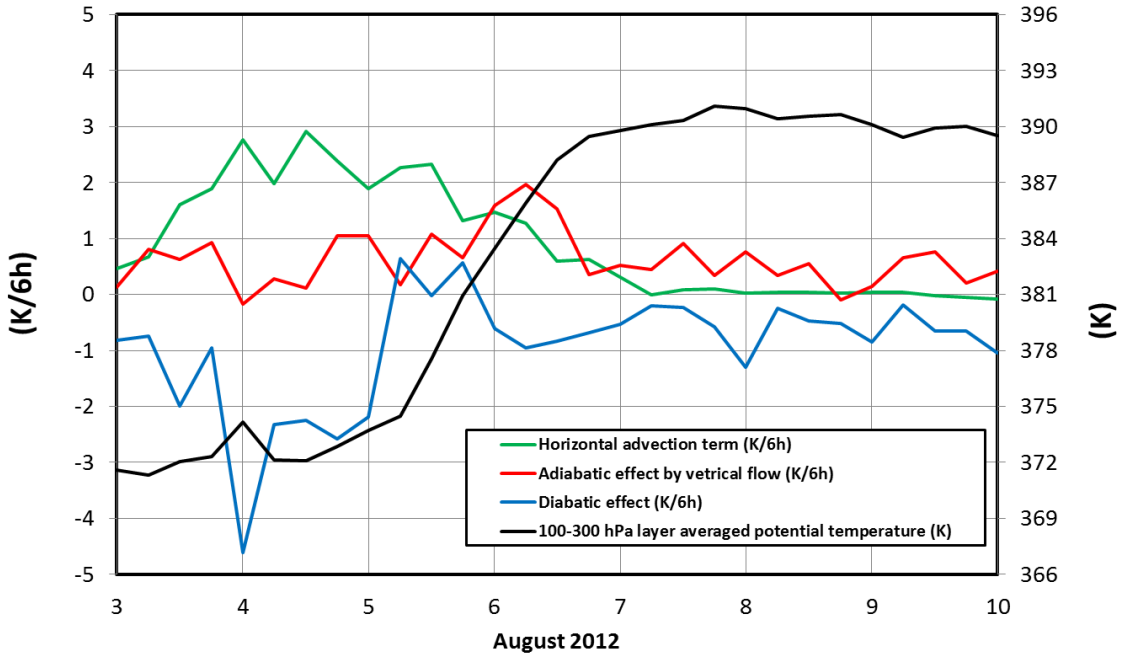

Fig. 21: Same as Fig.19, but for the case 2012.

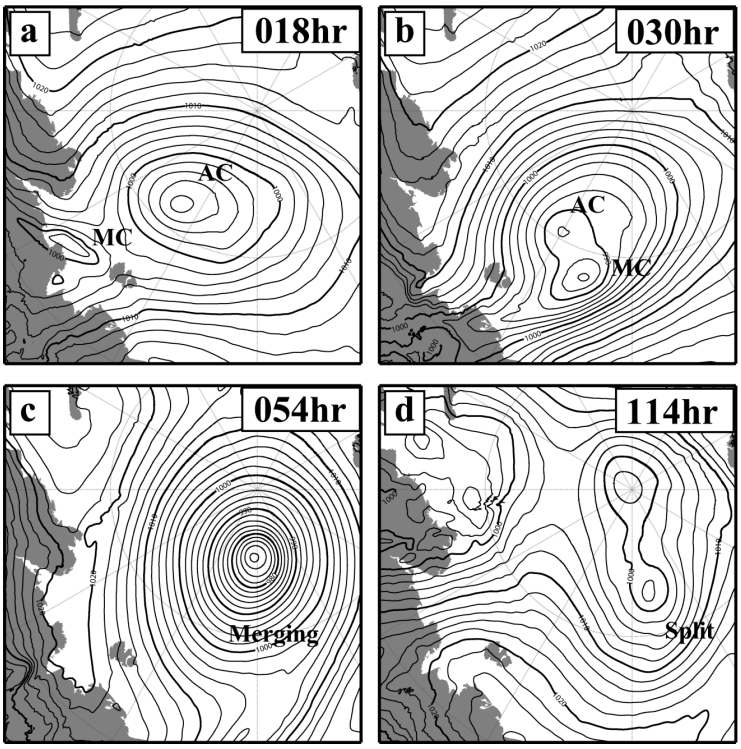

Fig. 22: Horizontal plots of the sea level pressure simulated by the NICAM at (a) 018 hr, (b) 030 hr, (c) 054 hr and (d) 114 hr. The intervals of thin and thick contours are 2 hPa and 10 hPa, respectively. A circle with letter "MC" indicates the mesoscale cyclone. The gray shade denotes the land.

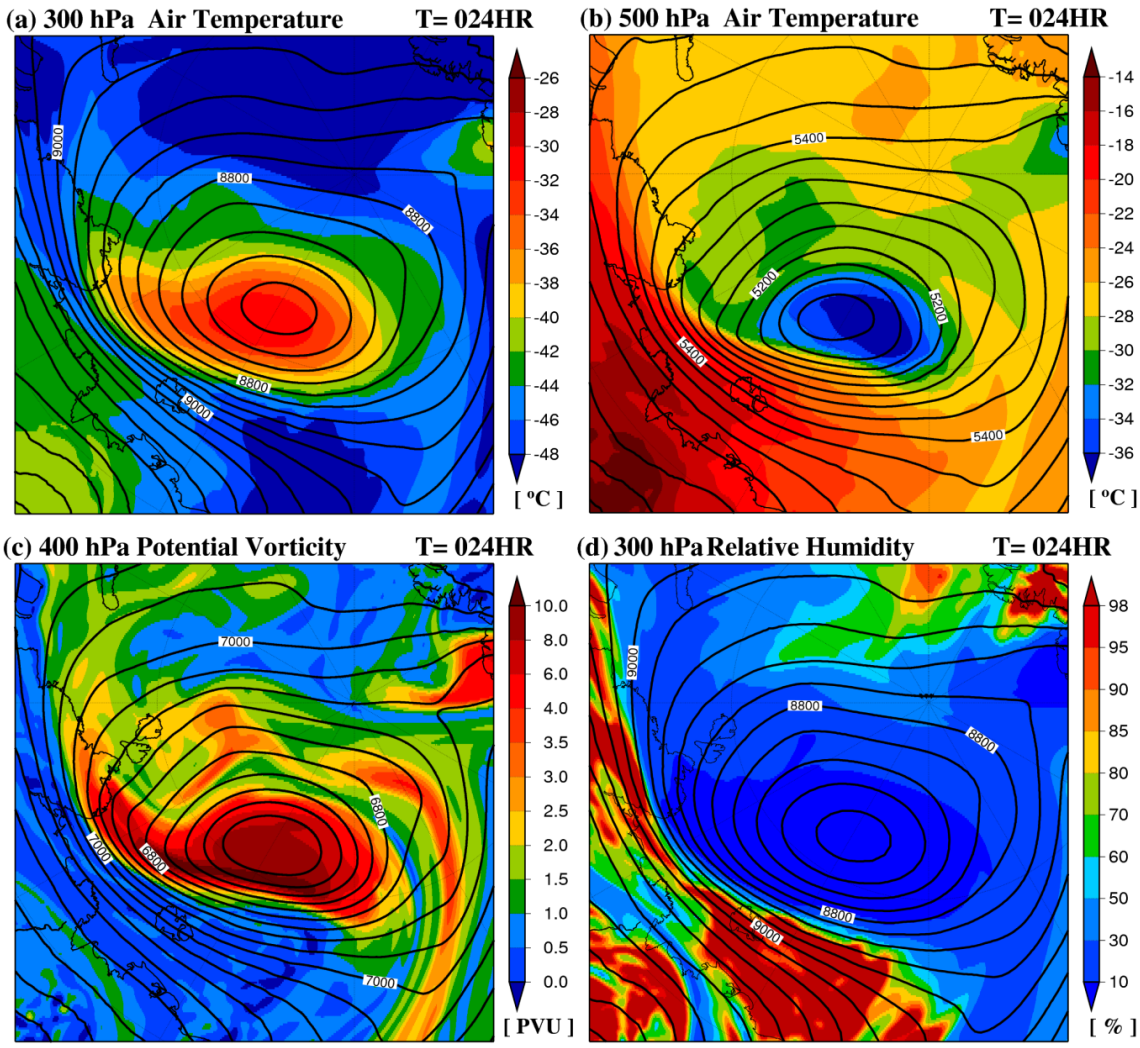

Fig. 23: Horizontal plots of (a) air temperature at 300 hPa, (b) air temperature at 500 hPa, (c) potential vorticity at 400 hPa and (d) relative humidity at 300 hPa simulated by NICAM at 024 hr. The geopotential height at the levels is described in each figure with contour interval of 40 m.

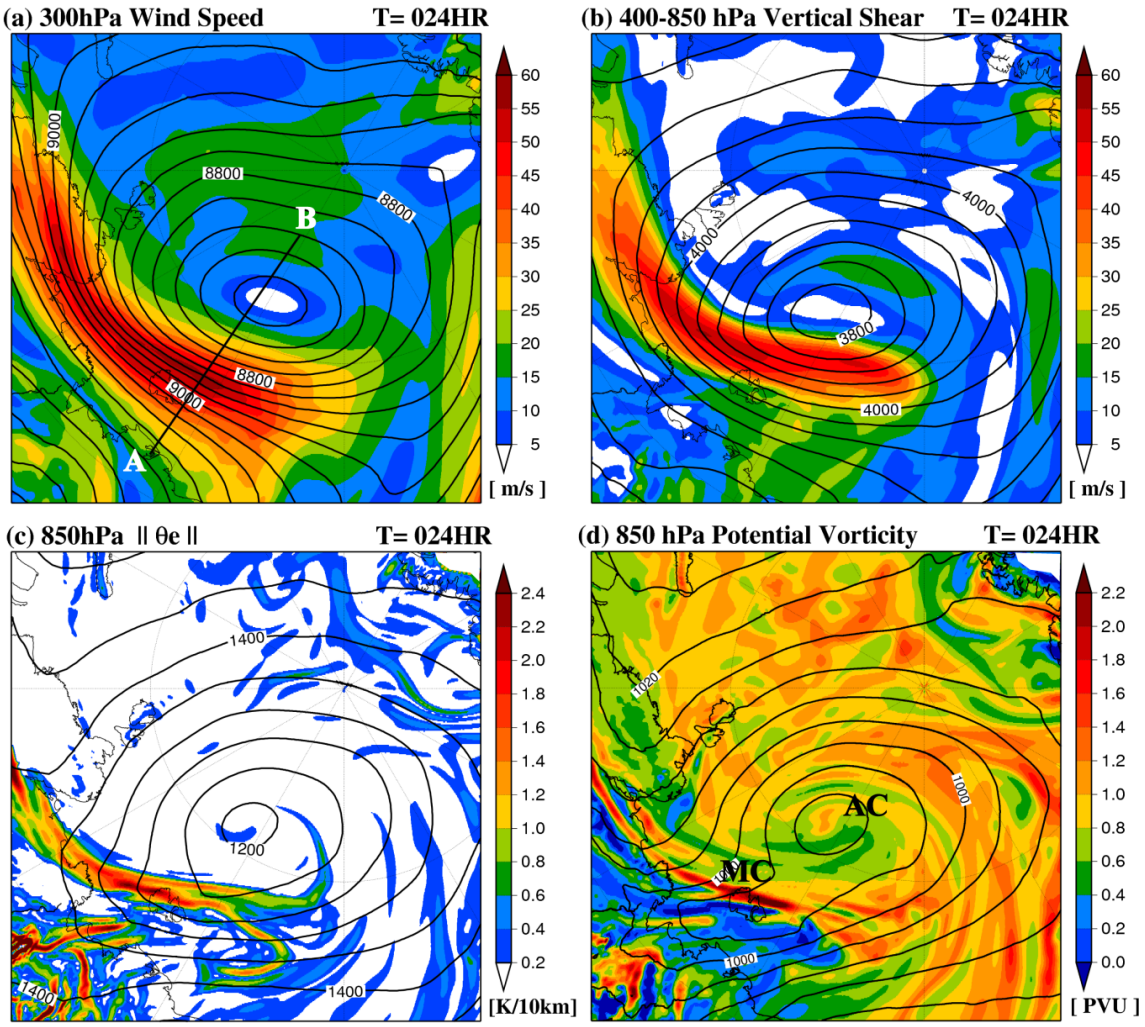

Fig. 24: Horizontal maps of (a) wind speed (m/s) at 300 hPa, (b) 400-850 hPa vertical wind shear (m/s), (c) magnitude of front (K/10 km) and (d) potential vorticity (PVU) at 850 hPa simulated by NICAM. The contours show the geopotential height each level (a - c) with the interval of 40 m and sea level pressure (d) with the interval of 4 hPa.

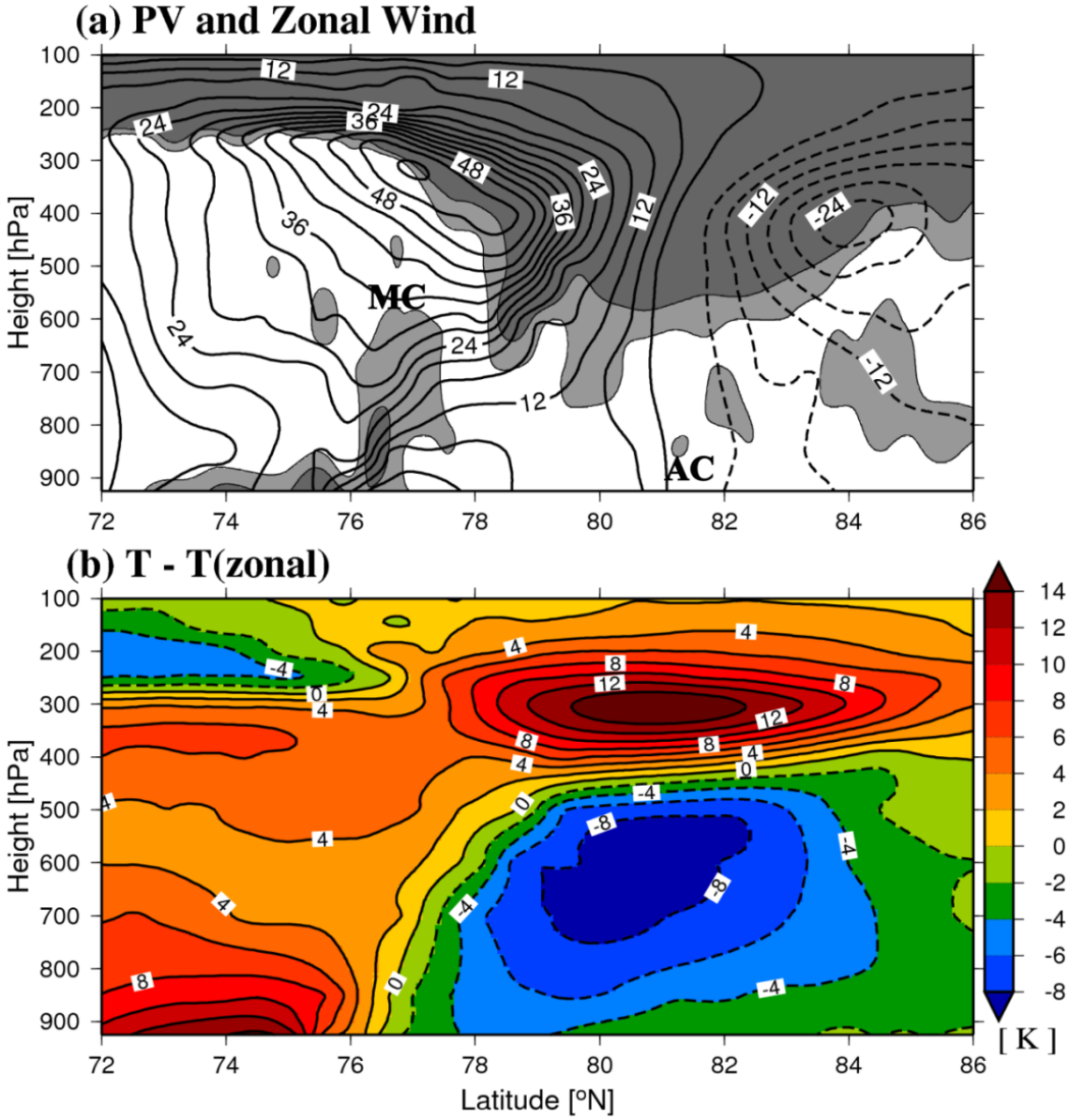

Fig. 25: Latitude-height cross sections along the AB line in figure 5 (a) of (a) potential vorticity (color, PVU) and zonal wind speed (contour, m/s) and (b) temperature deviation from zonal mean temperature (color and contour, K) simulated by NICAM at 024 hr. The light and heavy gray in (a) show the 1 PVU and the 2 PVU, respectively. The solid and dashed contours show the westerly and the easterly with the interval of 4 (m/s), respectively (a). The letters AC and MC indicate the latitudal locations of the centers of arctic cyclone and mesoscale cyclone, respectively.

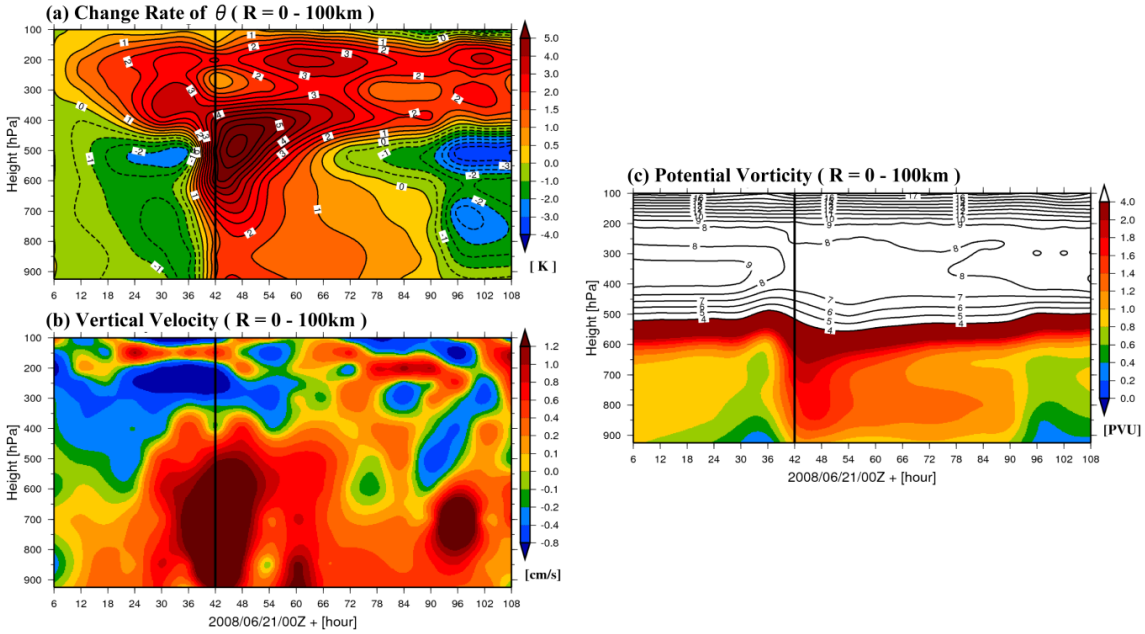

Fig. 26: Time-height cross sections of the regionally averaged (a) change rates of potential temperature (K), (b) vertical velocity (m/s) and (c) potential vorticity (PVU). The solid and dashed contours highlight the positive and negative, respectively in (a). In (c), the parts $\sim$ 4 (PVU) are displayed by colors and 4 $\sim$ (PVU) are indicated by contours with interval of 1.0. The thick black lines denote a time of the occurrence of vortex coupling.

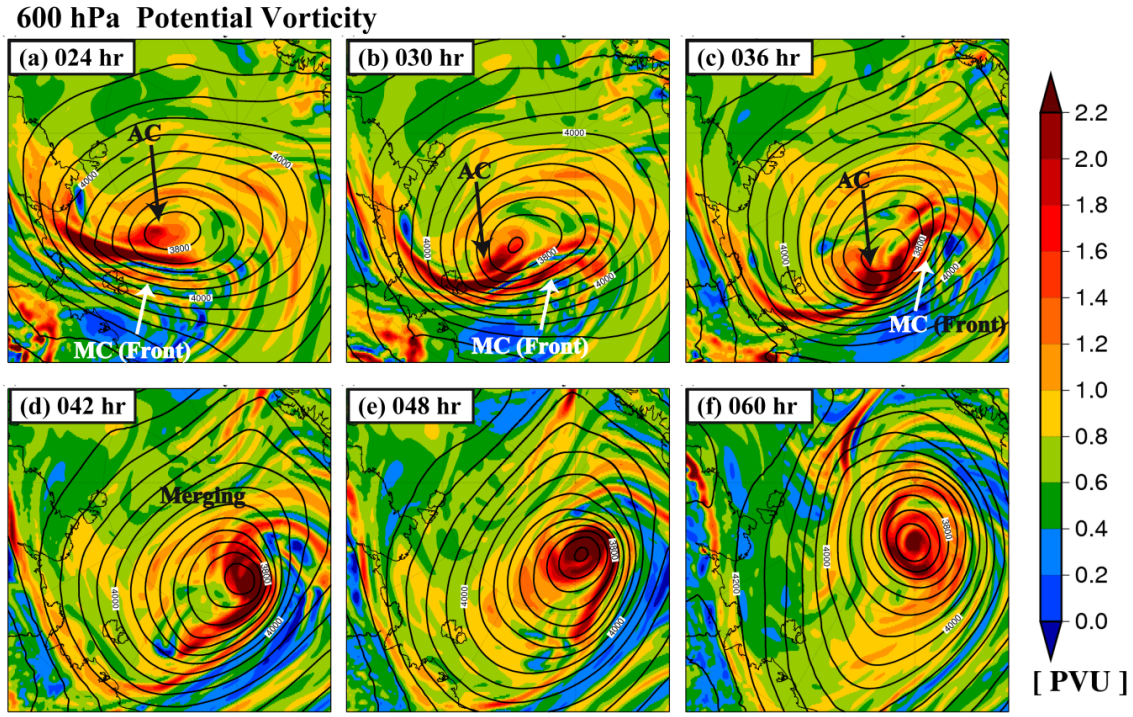

Fig. 27: Horizontal plots of potential vorticity (PVU) at 600 hPa at (a) 024 hr, (b) 030 hr, (c) 036 hr, (d) 042 hr, (e) 048 hr and (f) 060 hr simulated by NICAM. The geopotential height at 600 hPa is also illustrated in all figures with the interval of 40 m. The black arrows with a letter "AC" indicate the cores of high PV with the center of the AC and the write arrows with a letter "MC" indicate the spiral bands of high PV with the MC (Front).

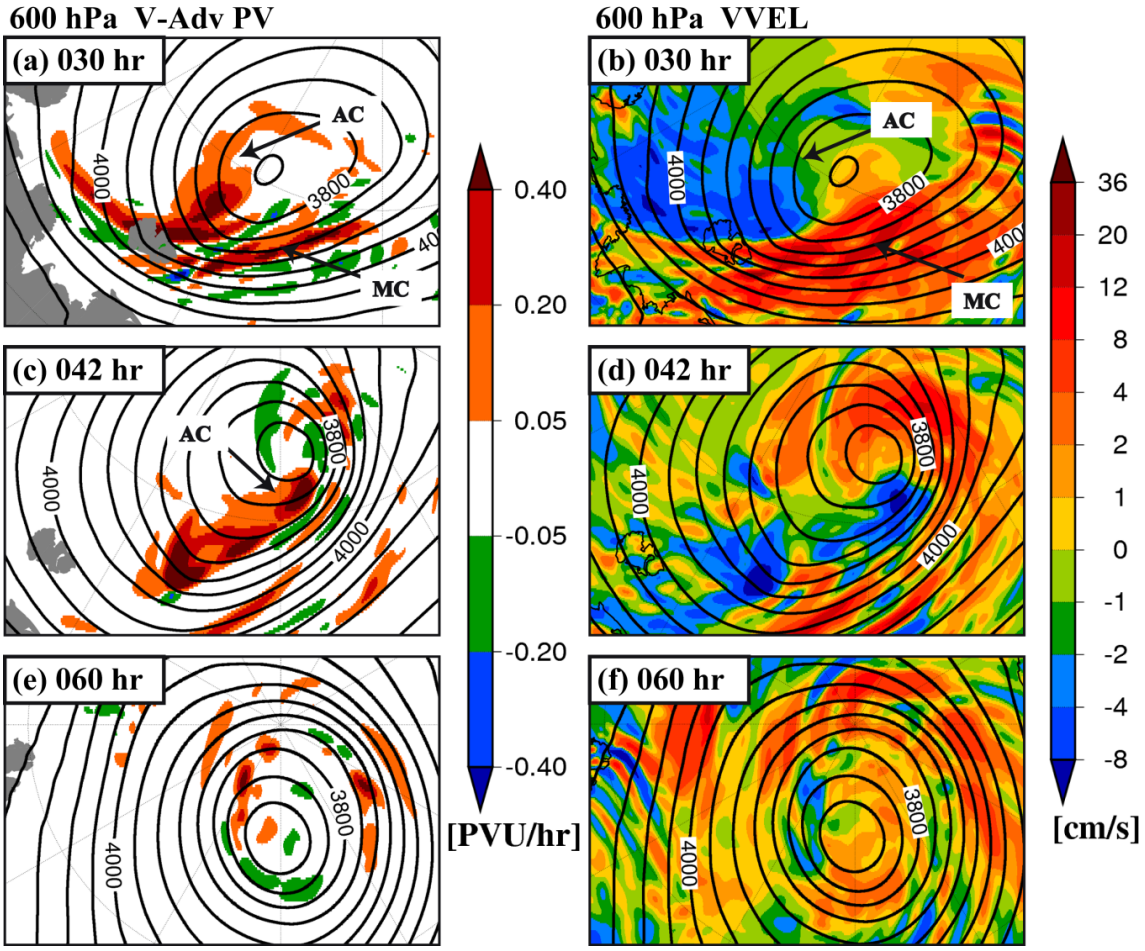

Fig. 28: Horizontal distributions at 600 hPa of (a) the vertical advection of potential vorticity tendency (PVU/hr) and (b) vertical velocity (cm/s) at 030 hr simulated by NICAM. Same as (a, b) but for 042 hr (c, d) and but for 060 hr (e, f). The geopotential height at 600 hPa is also illustrated in all figures with the interval of 40 m. An arrow with a letter "AC" indicates the PV generation by downdraft located at backside of the AC (a, c). An arrow with a letter "MC" indicates the PV generation by updraft by the MC (a, c).

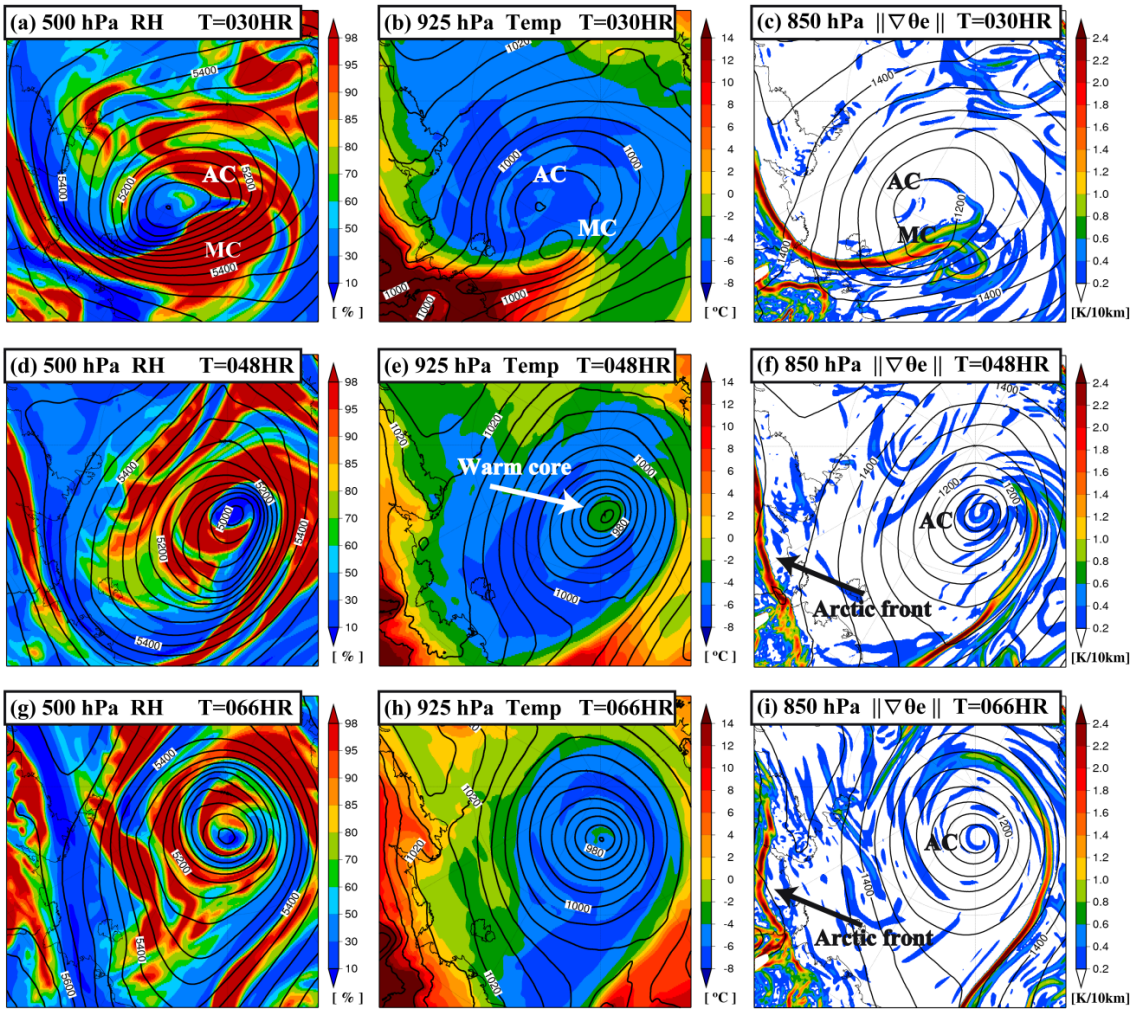

Fig. 29: Horizontal plots of (a) relative humidity (%) at 500 hPa, (b) air temperature (C) at 925 hPa and the magnitude of front (K/10 km) at 850 hPa at 024 hr simulated by NICAM. (d), (e) and (f) same as (a), (b) and (c) but for 048 hr. (g), (h) and (i) same as (a), (b) and (c) but for 066 hr. The geopotential height at 500 hPa, sea level pressure and the height at 850 hPa are also illustrated in (a, d, g), (b, e, h) and (c, f, i), respectively. A write arrow with a letter "Warm core" highlights the warm core (e). A black arrow with a letter "Arctic front" highlights the arctic front (f, i). The letters "AC" and "MC" highlight the arctic cyclone and mesoscale cyclone.

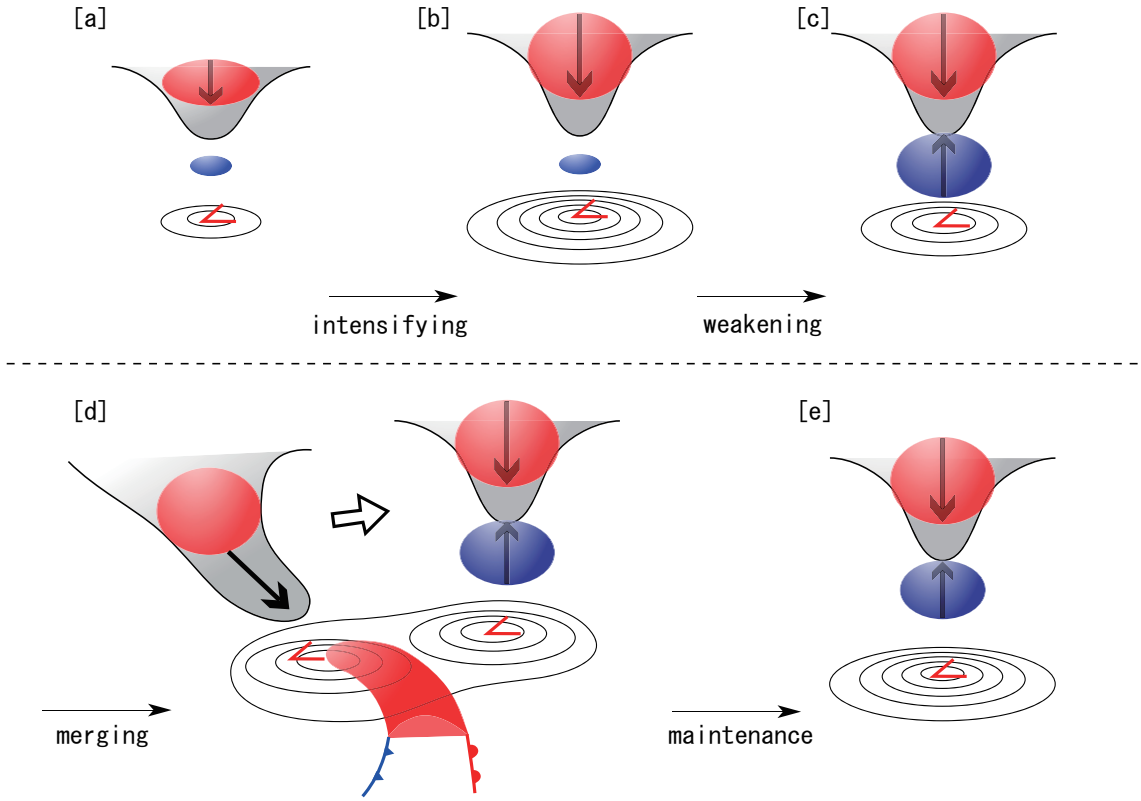

Fig. 30: Schematic diagram of the life cycle of the Arctic cyclones. The situation of the Arctic cyclone is in the (a) appearing stage, (b) mature stage, (c) dissipating stage, (d) merging stage with the frontal cyclone and (e) maintenance stage. The oval spheres with red color indicate the warm cores. And, the oval spheres with the blue color indicate cold cores. The bold solids with funnel shape indicate tropopause folding of the Arctic cyclone (a-e) and a baroclinic cyclone (d). The black arrows in the warm oval spheres indicate the lower stratospheric downdrafts which intensify the warm core. The black arrows in the cold oval spheres indicate the tropospheric downdrafts which produce the cold core. An arrow defined by outlines in (d) indicate the moving derection of the baroclinic cyclone. A black arrow in (d) is tropopause intrusion. A red line and a blue line in (d) indicate a warm front and a cold front of the baroclinic cyclone. The red L marks denote the cyclone centers.